

Faster Approximate Dynamic Programming by Freezing Slow States

Yijia Wang and Daniel R. Jiang

University of Pittsburgh

January 4, 2023

Abstract

We consider infinite horizon Markov decision processes (MDPs) with *fast-slow* structure, meaning that certain parts of the state space move “fast” (and in a sense, are more influential) while other parts transition more “slowly.” Such structure is common in real-world problems where sequential decisions need to be made at high frequencies, yet information that varies at a slower timescale also influences the optimal policy. Examples include: (1) service allocation for a multi-class queue with (slowly varying) stochastic costs, (2) a restless multi-armed bandit with an environmental state, and (3) energy demand response, where both day-ahead and real-time prices play a role in the firm’s revenue. Models that fully capture these problems often result in MDPs with large state spaces and large effective time horizons (due to frequent decisions), rendering them computationally intractable. We propose an approximate dynamic programming algorithmic framework based on the idea of “freezing” the slow states, solving a set of simpler finite-horizon MDPs (the *lower-level* MDPs), and applying value iteration (VI) to an auxiliary MDP that transitions on a slower timescale (the *upper-level* MDP). We also extend the technique to a function approximation setting, where a feature-based linear architecture is used. On the theoretical side, we analyze the regret incurred by each variant of our frozen-state approach. Finally, we give empirical evidence that the frozen-state approach generates effective policies using just a fraction of the computational cost, while illustrating that simply omitting slow states from the decision modeling is often not a viable heuristic.

1 Introduction

We consider sequential decision problems, modeled as Markov decision processes (MDPs), that are endowed with a new “fast-slow” structure: a *fast-slow* MDP has a state that can be divided into two parts, a *slow state* and a *fast state*. At each time step, the transition of the slow state results in a change that is relatively small compared to that of the fast state. An alternative view from the perspective of the reward function (rather than the transition function) is that the reward is less sensitive to changes in the slow state. Fast-slow structure is common in important real-world problems where sequential decisions need to be made at high frequencies, yet information that varies at a slower timescale also influences the optimal policy. The following examples illustrate this idea.

1. **Service allocation in multi-class queues.** The first example is a dynamic service allocation problem for a multi-class queue (Ansell et al., 2003; Brown and Haugh, 2017), with the addition of stochastic holding costs (i.e., the cost of leaving items in the queue) that vary slowly and can be viewed as the slow state (Lee and Vojnovic, 2021). One prominent motivation is the case of energy-aware job scheduling in data centers, where variations of electricity prices over time can influence the holding cost (Ren et al., 2012; Zhou et al., 2013; Mao et al., 2019).
2. **Restless multi-armed bandit with an environmental state.** Our second example application is the restless multi-armed bandit (Whittle, 1988; Weber and Weiss, 1990; Killian et al., 2021; Zhang and Frazier, 2021) with an environmental state, a model that is applicable to a problems ranging from machine maintenance (Smallwood and Sondik, 1973; Duan et al., 2018; Ruiz-Hernández et al., 2020) to dynamic assortment planning (Brown and Smith, 2020) to public health and preventative healthcare (Mate et al., 2020; Lee et al., 2019; Biswas et al., 2021). The restless bandit model involves making intervention decisions (e.g., whether to perform maintenance) on “arms” (e.g., machines), each of which is associated with an evolving internal state. Here, the environmental state can be viewed as the slow state, because it often transitions slowly relative to the arms’ internal states.
3. **Energy demand response.** We can also apply the fast-slow framework in sequential decision problems from the realm of demand response in the electricity market. Specifically, we consider the problem faced an energy aggregator who observes a day-ahead price and then

simultaneously bids a reduction quantity into the demand response market and sets the compensation for demand reduction from consumers (Albadi and El-Saadany, 2008; Eid et al., 2016; Khezeli and Bitar, 2017; Khezeli et al., 2017; Wang et al., 2018). Essentially, the aggregator hopes to generate profit from the difference between the contracted price for delivery of demand reduction to the market and the price that offers customers for that reduction. However, the aggregator has to consider the demand elasticity of its customers, along with the stochasticity of day-ahead prices and real-time prices (which determine the “penalty” for mismatch between the promised and realized quantities of demand reduction). Since real-time prices are much more volatile compared to the day-ahead prices, it is reasonable to view day-ahead prices as the slow state.

Attempts to optimally solve a model that incorporates the full state space along with the true decision-making frequency often encounter computational issues, due to the challenge of solving an MDP with a large state space over a large number of periods. Anecdotal evidence suggests that to improve tractability, both practitioners and academic researchers may elect to design simplified decision models that *ignore* the effect of the slow state on components of their problems. In other words, these states might be intentionally left out of the state variable by, e.g., fixing them to constant values. Although such an approach results in policies that can be obtained in a computationally tractable manner, we see in Section 9 that they can incur significant regret compared to the optimal policy.

1.1 Main Contributions

In this paper, we propose somewhat of a compromise between the solving the full MDP and completely ignoring slow states, by designing a framework around periodically “freezing” and “releasing” slow states, and re-using policies that are computed based on a frozen slow-state model. Specifically, we make the following contributions:

1. We first consider a fast-slow MDP and provide an (exact) reformulation into an MDP with hierarchical structure. The *upper level* is a slow-timescale infinite horizon MDP and the *lower level* is a fast-timescale finite horizon MDP with T periods. One period of the upper-level problem is composed of a complete lower-level problem. We propose a *frozen-state*

approximation to the reformulated MDP, along with an associated *frozen-state value iteration* (FSVI) algorithm, where the slow state is frozen in the lower-level problem, while each period in the upper-level problem “releases” the slow state. Computational benefits arise in several ways: (1) re-use of the lower-level policy (which is computed once) when applying value iteration in the upper level, (2) frozen states simplify the dynamics of the lower-level MDP (dramatically fewer successor states), and (3) the lower-level MDP thus becomes separable into independent MDPs, opening the door to speedups via parallel computation. Solving the frozen-state approximation gives a policy that switches between the one action from upper-level policy and $T - 1$ actions from the lower-level policy. We give a theoretical analysis that upper bounds the expected regret from applying this policy compared to the optimal policy.

2. We then discuss an additional step of approximation that further reduces computational requirements, called the *nominal-state approximation*, which takes advantage of a factored reward function assumption and approximates the lower-level MDP using a fixed set of “nominal” slow states. The consequence is that instead of solving the lower-level MDP for all slow states, this approximation allows us to solve it only for the set of nominal slow states, which are then used to approximate the lower-level value for other slow states. We also provide an upper bounds on the expected regret of the policy obtained from the nominal state approximation.
3. Next, we show how the fast-slow framework can also be exploited in an approximate dynamic programming (ADP) setting (Bertsekas and Tsitsiklis, 1996; Powell, 2007). Specifically, we design a *frozen-state approximate value iteration* (FSAVI) algorithm that mimics FSVI but uses a linear architecture to approximate the value function in both the lower and upper levels. The linear architecture combines estimated values from a set of pre-selected states to form approximations of the value function at other states, based on the technique introduced in Tsitsiklis and Van Roy (1996). We provide an analysis of the expected regret for policies generated by FSAVI.
4. Lastly, we perform a systematic empirical study on three problem settings (service allocation in multi-class queues, restless bandit with an environmental state, and energy demand response). We show that the proposed algorithms based on the frozen-state approximation quickly converge to good policies using significantly less computation compared to standard

methods (value iteration, approximate value iteration, Q-learning, deep Q-networks, and a baseline that ignores slow states). Notably, our results show that ignoring the slow state leads particularly poor results. We also give qualitative evidence that policies generated by the frozen-state approach have structural features resembling those of the optimal policy.

2 Related Work

In this section, we provide a brief review of related literature. First, there exists a stream of literature focused on sequential decision making problems with *exact* hierarchical, multi-timescale structure. [Chang et al. \(2003\)](#) study multi-timescale MDPs, which are composed of M different decisions that are made on M different discrete timescales. The authors consider the impact of upper-level states and actions on the transition of the lower levels, an idea is also present in our fast-slow framework. Multi-timescale MDPs have often been applied in supply chain problems, including production planning in semiconductor fabrication ([Panigrahi and Bhatnagar, 2004](#); [Bhatnagar and Panigrahi, 2006](#)), hydropower portfolio management ([Zhu et al., 2006](#)), and strategic network growth for reverse supply chains ([Wongthatsanekorn et al., 2010](#)). [Wang et al. \(2018\)](#) propose a row-generation-based algorithm to solve a linear programming formulation of the multi-timescale MDP. [Jacobson et al. \(1999\)](#) consider “piecewise stationary” MDPs, where the transition and reward functions are “renewed” every $N + 1$ periods, motivated by problems where routine decisions are periodically interrupted by higher-level decisions. For the case of large renewal periods, they propose a policy called the “initially stationary policy” which uses a fixed decision rule for some number of initial periods in each renewal cycle. Our fast-slow model focuses on a novel fast-slow structure present in many MDPs and unlike the above work, *does not assume* any natural/exact hierarchical structure. Instead, we focus on how a particular type of (frozen-state) hierarchical structure can be used as an *approximation* to the true MDP. However, we note that many MDPs with natural two-timescale structure can also fit into our framework, and therefore, given that perspective, our model can be viewed as a generalization.

Our proposed frozen-state algorithms are also related to literature on *hierarchical reinforcement learning*, which are methods that artificially decompose a complex problem into smaller sub-problems ([Barto and Mahadevan, 2003](#)). Approaches include the options framework ([Sutton et al., 1999](#)), the hierarchies of abstract machines (HAMs) approach ([Parr and Russell, 1998](#)), and MAXQ

value function decomposition (Dietterich, 2000).

Out of these three approaches, the options framework is most closely related to this paper. A *Markov option* (also called a *macro-action* or *temporally extended action*) is composed of a policy, a termination condition, and an initiation set (Sutton et al., 1999; Precup, 2000). One of the biggest challenges is to automatically construct options that can effectively speed up reinforcement learning. A large portion of work in this direction is based on *subgoals*, states that might be beneficial to reach (Digney, 1998; McGovern and Barto, 2001; Jonsson and Barto, 2005; Ciosek and Silver, 2015; Wang et al., 2022). The subgoals are identified by utilizing the learned model of the environment (Menache et al., 2002; Mannor et al., 2004; Şimşek and Barto, 2004; Şimşek et al., 2005), or through trajectories without learning a model (McGovern and Barto, 2001; Stolle and Precup, 2002). The options (and subgoals) framework is largely motivated by robotics and navigation-related tasks, while we are particularly interested in solving problems that arise in the operations research and operations management domains. The problems that we study do not decompose naturally into “subgoals” — leading us to identify and focus on the fast-slow structure, which does indeed arise naturally for many problems of interest.

Another work that is related to the options framework is Song and Xu (2020), who divide finite-horizon MDPs into two sub-problems along the time horizon, and concatenate their optimal solutions to generate an overall solution. Our paper also, in a sense, divides MDPs along the time horizon, but our work is quite different from Song and Xu (2020) in that we work on *infinite horizon problems* and convert them into auxiliary problems that operate on a *slower timescale*, which takes advantage of reusable lower-level policies. More importantly, the various methods we propose all build on the idea of freezing certain states to reduce computational cost, which is unique to our approach and to our knowledge, this is a novel direction that has not been proposed before.

3 Fast-Slow MDPs

In this section, we introduce the *base model*, the original MDP to be solved and formally introduce the notion of a *fast-slow* MDP. We then provide a hierarchical reformulation of the base model using fixed-horizon policies, and show the equivalence (in optimal value) between the two models.

3.1 Base Model

Consider a discrete-time MDP $\langle \mathcal{S}, \mathcal{A}, \mathcal{W}, f, r, \gamma \rangle$, where \mathcal{S} is the finite state space, \mathcal{A} is the finite action space, \mathcal{W} is the space of possible realizations of an exogenous, independent and identically distributed (i.i.d.) noise process $\{w_t\}$ defined on a discrete probability space $(\Omega, \mathcal{F}, \mathbb{P})$, $f : \mathcal{S} \times \mathcal{A} \times \mathcal{W} \rightarrow \mathcal{S}$ is the transition function, $r : \mathcal{S} \times \mathcal{A} \rightarrow [0, r_{\max}]$ is the bounded reward function, and $\gamma \in [0, 1)$ is the discount factor for future rewards (Puterman, 2014). The objective is

$$U^*(s) = \max_{\{\nu_t\}} \mathbb{E} \left[\sum_{t=0}^{\infty} \gamma^t r(s_t, \nu_t(s_t)) \mid s_0 = s \right], \quad (1)$$

where states transition according to $s_{t+1} = f(s_t, a_t, w_{t+1})$ and we optimize over sequences of policies $\nu_t : \mathcal{S} \rightarrow \mathcal{A}$, which are deterministic mappings from states to actions. The expectation is taken over exogenous noise process $\{w_t\}_{t=1}^{\infty}$. We assume throughout that \mathcal{S} , \mathcal{A} , \mathcal{X} , \mathcal{Y} , $\mathcal{S} \times \mathcal{A}$, and $\mathcal{X} \times \mathcal{Y}$ are equipped with the Euclidean metric,¹ which is naturally the case for many applications.

Assumption 1 (Separability and the Fast-Slow Property). *Suppose the following hold:*

(i) *The state space \mathcal{S} is separable and can be written as $\mathcal{S} = \mathcal{X} \times \mathcal{Y}$. We call \mathcal{X} the “slow state space” and \mathcal{Y} the “fast state space.”*

(ii) *Let $s_t = (x_t, y_t) \in \mathcal{S}$, where $x_t \in \mathcal{X}$ is the slow state and $y_t \in \mathcal{Y}$ the fast state, $a_t \in \mathcal{A}$, and $w_{t+1} \in \mathcal{W}$. The transition dynamics $s_{t+1} = f(s_t, a_t, w_{t+1}) \in \mathcal{S}$ can be written with the notation:*

$$x_{t+1} = f_{\mathcal{X}}(x_t, y_t, a_t, w_{t+1}) \in \mathcal{X} \quad \text{and} \quad y_{t+1} = f_{\mathcal{Y}}(x_t, y_t, a_t, w_{t+1}) \in \mathcal{Y},$$

for some $f_{\mathcal{X}} : \mathcal{S} \times \mathcal{A} \times \mathcal{W} \rightarrow \mathcal{X}$ and $f_{\mathcal{Y}} : \mathcal{S} \times \mathcal{A} \times \mathcal{W} \rightarrow \mathcal{Y}$.

(iii) *For any state $(x, y) \in \mathcal{S}$, action $a \in \mathcal{A}$, and exogenous noise $w \in \mathcal{W}$, suppose the one-step transitions of x and y satisfy:*

$$\|y - f_{\mathcal{Y}}(x, y, a, w)\|_2 \leq d_{\mathcal{Y}} \quad \text{and} \quad \|x - f_{\mathcal{X}}(x, y, a, w)\|_2 \leq \alpha d_{\mathcal{Y}},$$

¹However, as long as the relevant spaces are metric spaces, the framework continues to hold. We choose Euclidean metrics as they are natural for our applications.

for some $d_Y < \infty$ and $\alpha \in [0, 1]$.

Remark 1. Note that one particularly instructive example is the case of exogenous slow states, where $x_{t+1} = f_X(x_t, w_{t+1})$. Here, the transition does not depend on the action a_t , nor does it depend on the fast state y_t . Such a model is common in practice: examples of exogenous slow states include prices, weather conditions, and other environmental variables that are not influenced by the decision maker’s actions or the states of the primary system. See, e.g., [Yu and Mannor \(2009\)](#), who study a related model called the “arbitrarily modulated MDP.”

Assumption 2 (Lipschitz Properties). Suppose that the reward function r , transition function f , and optimal value function U^* are Lipschitz with respect to $\|\cdot\|_2$:

$$|r(s, a) - r(s', a')| \leq L_r \|(s, a) - (s', a')\|_2, \quad (2)$$

$$\|f(s, a, w) - f(s', a', w)\|_2 \leq L_f \|(s, a) - (s', a')\|_2, \quad (3)$$

$$\|U^*(s) - U^*(s')\|_2 \leq L_U \|s - s'\|_2, \quad (4)$$

for some Lipschitz constants L_r , L_f , and L_U . Lipschitz assumptions are common in the literature; see, for example, [Ok et al. \(2018\)](#), [Domingues et al. \(2021\)](#), [Sinclair et al. \(2020\)](#), and [Sinclair et al. \(2022\)](#). In [Appendix F](#), we give bounds on L_U in terms of L_r and L_f . While we could have used those results directly and omitted the assumption on L_U , we opt to include [\(4\)](#) to increase the clarity of our results.

Definition 1 (Fast-Slow MDP). An MDP $\langle \mathcal{S}, \mathcal{A}, \mathcal{W}, f, r, \gamma \rangle$ is called a (α, d_Y) -fast-slow MDP if [Assumptions 1](#) and [2](#) are satisfied.

Given any state $s = (x, y)$, noise w , and policy ν , we use the notation $f^\nu(s, w) = f(s, \nu(s), w)$, $f_X^\nu(x, y, w) = f_X(x, y, \nu(x, y), w)$, $f_Y^\nu(x, y, w) = f_Y(x, y, \nu(x, y), w)$, and $r(x, y, \nu) = r(x, y, \nu(x, y))$ throughout the paper. The value of a stationary policy² ν at state (x, y) is the expected cumulative reward starting from state (x, y) following policy ν , i.e.,

$$U^\nu(x, y) = \mathbb{E} \left[\sum_{t=0}^{\infty} \gamma^t r(x_t, y_t, \nu) \mid (x_0, y_0) = (x, y) \right] = r(x, y, \nu) + \gamma \mathbb{E}[U^\nu(x', y')],$$

²It is well-known that there exists an optimal policy to [\(1\)](#) that is both stationary and deterministic. See [Puterman \(2014\)](#).

where $(x', y') = f^\nu(x, y, w)$ and $(x_{t+1}, y_{t+1}) = f^\nu(x_t, y_t, w_t)$ for all t . The optimal value function at state $U^*(x, y)$, as defined in (1), satisfies the Bellman equation, i.e.,

$$U^*(x, y) = \max_a r(x, y, a) + \gamma \mathbb{E}[U^*(x', y')]. \quad (5)$$

Denote by H the Bellman operator of the base model; for any state (x, y) and value function U ,

$$(HU)(x, y) = \max_a r(x, y, a) + \gamma \mathbb{E}[U(f(x, y, a, w))]. \quad (6)$$

A policy that is greedy with respect to the optimal value function, i.e.,

$$\nu^*(x, y) = \arg \max_a r(x, y, a) + \gamma \mathbb{E}[U^*(x', y')].$$

is an optimal policy, and the optimal value U^* and the value of the optimal policy U^{ν^*} are the same.

3.2 Hierarchical Reformulation using Fixed-Horizon Policies

In this section, we derive an exact hierarchical reformulation with the original timescale broken up into groups of T periods each. The reformulation holds for a general MDP $\langle \mathcal{S}, \mathcal{A}, \mathcal{W}, f, r, \gamma \rangle$, but the concepts that we introduce in this section will serve as the basis for developing our frozen-state computational approach for fast-slow MDPs.

Denote $(\mu, \boldsymbol{\pi})$ a T -horizon policy, which is a sequence of T policies $(\mu, \pi_1, \dots, \pi_{T-1})$, $\mu : \mathcal{S} \rightarrow \mathcal{A}$, $\pi_t : \mathcal{S} \rightarrow \mathcal{A}$ and $\boldsymbol{\pi} = (\pi_1, \dots, \pi_{T-1})$. Following $(\mu, \boldsymbol{\pi})$ means that we take the first action according to μ and then next $T - 1$ actions according to $\boldsymbol{\pi}$. Given any state s_0 , the T -period reward function (of the base model) associated with $(\mu, \boldsymbol{\pi})$ is written as:

$$R(s_0, \mu(s_0), \boldsymbol{\pi}) = r(s_0, \mu) + \sum_{t=1}^{T-1} \gamma^t r(s_t, \pi_t), \quad (7)$$

where $s_1 = f^\mu(s_0, w_1)$ and $s_{t+1} = f^{\pi_t}(s_t, w_{t+1})$ for $t > 0$.

A T -periodic policy $(\mu, \boldsymbol{\pi})$ refers to the infinite sequence that repeatedly applies the T -horizon policy $(\mu, \boldsymbol{\pi})$, i.e., $(\mu, \boldsymbol{\pi}, \mu, \boldsymbol{\pi}, \dots)$. Note that despite it not being a stationary policy, the T -periodic policy $(\mu, \boldsymbol{\pi})$ can be implemented in the infinite horizon problem defined in (1). The value of the

T -periodic policy $(\mu, \boldsymbol{\pi})$ at state s_0 is

$$\bar{U}^\mu(s_0, \boldsymbol{\pi}) = \mathbb{E} \left[\sum_{k=0}^{\infty} \gamma^{kT} R(s_k, \mu(s_k), \boldsymbol{\pi}) \mid s_0 = s \right] = \mathbb{E} [R(s_0, \mu(s_0), \boldsymbol{\pi}) + \gamma^T \bar{U}^\mu(s_T, \boldsymbol{\pi})],$$

where, again, $s_1 = f^\mu(s_0, w_1)$ and $s_{t+1} = f^{\pi_t}(s_t, w_{t+1})$ for $t > 0$ within each cycle of T periods. Figure 1 compares stationary policy ν and a T -periodic policy $(\mu, \boldsymbol{\pi})$ for the case of $T = 4$. In the figure, we also illustrate how rewards can be written in an ‘‘aggregated’’ fashion over the T periods using (7).

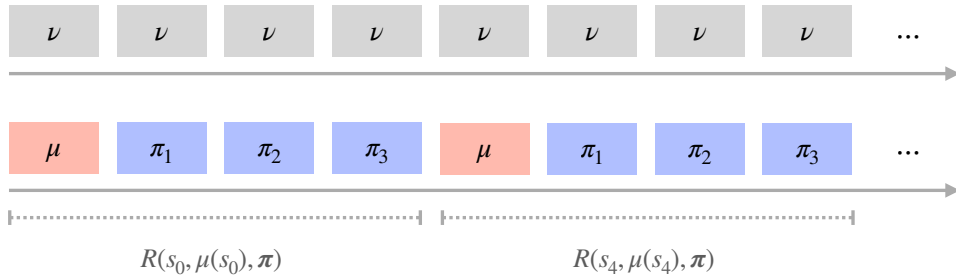


Figure 1: Illustration of a stationary policy μ (upper timeline) and a T -periodic policy $(\mu, \boldsymbol{\pi})$ (lower timeline) for $T = 4$. The periods covered by the T -period reward associated with $(\mu, \boldsymbol{\pi})$ is shown in the lower timeline.

The optimal value function satisfies the following Bellman equation:

$$\bar{U}^*(s_0) = \max_{(\mu, \boldsymbol{\pi})} \mathbb{E} [R(s_0, \mu(s_0), \boldsymbol{\pi}) + \gamma^T \bar{U}^*(s_T)], \quad (8)$$

where the ‘‘action’’ now involves selecting the $\boldsymbol{\pi}$ as well. Denote $(\mu^*, \boldsymbol{\pi}^*)$ an optimal T -periodic policy, which solves (8). In Proposition 3.1, we prove that the base model (5) and the hierarchical reformulation (8) are equivalent in a certain sense.

Proposition 3.1. *Given an MDP $\langle \mathcal{S}, \mathcal{A}, \mathcal{W}, f, r, \gamma \rangle$, the following hold:*

- (i) *The optimal value of the base model (5) is equal to the optimal value of the hierarchical reformulation (8), i.e., $U^* = \bar{U}^*$.*
- (ii) *An optimal stationary policy ν^* with respect to the base model (5) is also an optimal policy for the hierarchical reformulation (8), i.e., $\bar{U}^* = \bar{U}^{\nu^*}$.*

Proof. See Appendix A.2. □

Part (i) of Proposition 3.1 is most relevant to our situation in the sense that the optimal T -periodic policy (μ^*, π^*) is no better than the stationary optimal policy ν^* . Therefore, solving the hierarchical reformulation (8) allows us to achieve the same value as the ν^* , the optimal policy to the original base model (5).

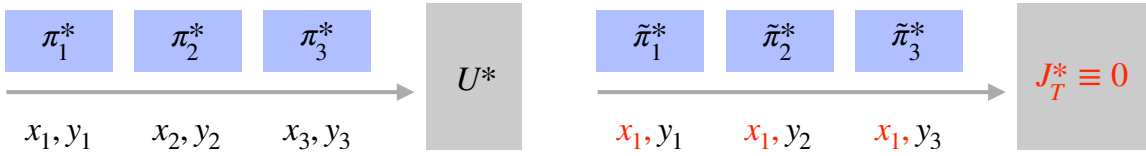
Note that, at this point, we have simply reformulated the problem, but (8) is no easier to solve than (5). Despite the more favorable discount factor γ^T in (8), its action space is now effectively the space of T -horizon policies, rather than a single action a . In the next section, we propose an approximation that allows us to *fix* a lower-level policy π and only optimize μ . This allows us to enjoy the γ^T discount factor while maintaining the same action space.

4 The Frozen-State Approximation

We propose a *frozen-state approximation*, where we make two simplifications to the T -period finite-horizon problem with terminal value U^* that is embedded in each T -period “time step” of (8), termed the *lower-level problem*. First, motivated by the slow transitions of x given in Assumption 1, we “freeze” slow states for all T periods of the lower-level problem, and second, we decouple the problem from the main MDP by solving an approximation with zero terminal value instead of U^* .

The first simplification reduces the computation needed to solve the finite-horizon MDP, while the second simplification, due to the decoupling from the main problem, allows us to *pre-compute* an approximation to π^* , which we denote $\tilde{\pi}^*$. By then fixing $\tilde{\pi}^*$, we are able to construct an auxiliary problem that proceeds at a timescale that is a factor of T *slower* than the MDP of the base model (equivalently, the discount factor becomes γ^T instead of γ), yet optimizing over the same action space. This naturally leads to ADP algorithms with computational benefits (see Sections 6, 7, and 8). The number of periods T to freeze the state is a parameter to the approach. See Figure 2 for a high-level illustration; we provide a detailed description of the approach in the next few sections.

Remark 2. *It is important to note that the freezing of states only occurs “within the algorithm” as a step toward more efficient computation of policies. Our resulting policies are then implemented in the underlying base model MDP, which proceeds naturally according to its true dynamics. Our theoretical and empirical results always attempt to answer the question: how well does a approximate policy, which is computed by pretending certain states are frozen, perform in the true model?*



(a) The lower-level problem (i.e., optimizing over π) embedded in (8). (b) The lower-level problem of the frozen-state approximation, with frozen x_1 and J_T^* instead of U^* .

Figure 2: A comparison of the lower-level problem of the hierarchical reformulation vs the lower-level problem of the frozen-state approximation.

4.1 The Lower-Level MDP (Frozen Slow States)

We view the problem from period 1 to period T as the “lower level” of the frozen-state approximation.³ To form the lower-level problem of the frozen-state approximation, we consider this $T - 1$ period problem in isolation:

$$J_1^{\tilde{\pi}}(x, y) = \mathbb{E} \left[\sum_{t=1}^{T-1} \gamma^{t-1} r(x_1, y_t, \tilde{\pi}_t) \mid (x_1, y_1) = (x, y) \right] \quad \text{and} \quad J_1^*(x, y) = \max_{\tilde{\pi}} J_t^{\tilde{\pi}}(x, y) \quad (9)$$

where $x_{t+1} = x_t = x$ remains frozen, $y_{t+1} = f_y^{\tilde{\pi}_t}(x, y_t, w_{t+1})$, and $\tilde{\pi} = (\tilde{\pi}_1, \dots, \tilde{\pi}_{T-1})$. The problem (9) can be solved using finite-horizon dynamic programming: accordingly, let the terminal $J_T^* \equiv 0$ and for $t = 1, 2, \dots, T - 1$, let

$$J_t^*(x, y) = \max_a r(x, y, a) + \gamma \mathbb{E}[J_{t+1}^*(x, y')], \quad (10)$$

where $y' = f_y(x, y, a, w)$. We also have the standard recursion for the performance of a policy:

$$J_t^{\tilde{\pi}}(x, y) = r(x, y, \tilde{\pi}_t(x, y)) + \gamma \mathbb{E}[J_t^{\tilde{\pi}}(x, f_y^{\tilde{\pi}_t}(x, y, w_{t+1}))], \quad (11)$$

with $J_T^{\tilde{\pi}} \equiv 0$. We denote by \tilde{H} the Bellman operator of the lower-level problem, which is on the same timescale as the base model (hence, the discount factor is γ) and looks similar to the Bellman operator H defined in (6), but the transition of the slow-state x is frozen. For any state (x, y) and

³This corresponds to the periods relevant to π from (μ, π) in the hierarchical reformulation (8), whose structure the frozen-state approximation mimics.

lower-level value function J_{t+1} ,⁴ define:

$$(\tilde{H}J_{t+1})(x, y) = \max_a r(x, y, a) + \gamma \mathbb{E}[J_{t+1}(x, f_Y(x, y, a, w))]. \quad (12)$$

Note that (12) can be viewed as an approximation to (6). Analogously, let $\tilde{H}^{\tilde{\pi}}$ be the Bellman operator associated with (11).

Also, let $\tilde{\pi}^* = (\tilde{\pi}_1^*, \dots, \tilde{\pi}_{T-1}^*)$ be the finite-horizon policy that is greedy with respect to J_t^* :

$$\tilde{\pi}_t^*(x, y) = \arg \max_a r(x, y, a) + \gamma \mathbb{E}[J_{t+1}^*(x, y')].$$

It may not immediately be clear why freezing slow states is desired. There are two main computational benefits to solving (10) instead of an analogous version of (10) *without* freezing x :

- In algorithms like value iteration (Puterman, 2014), each update requires computing expectations over successor states, and therefore the number of successor states impacts the number of operations for each step of value iteration. When x is frozen, the number of successor states is much smaller since we only have successor fast states (y'): in other words, we only need to compute $\mathbb{E}[J_{t+1}^*(x, y')]$ instead of $\mathbb{E}[J_{t+1}^*(x', y')]$.⁵
- Second, (10) can effectively be viewed as $|\mathcal{X}|$ independent MDPs, one for each $x \in \mathcal{X}$, allowing for the possibility of computing the policy with additional parallelism. In the nominal-state approximation discussed Section 7, we analyze the error of an approach that solves only a small number out of the $|\mathcal{X}|$ independent MDPs.

4.2 The Upper-Level MDP (True State Dynamics)

Let us now consider the upper-level problem of the frozen-state approximation, which is an infinite horizon problem with groups of T periods aggregated. Denote the stationary upper-level policy by $\mu : \mathcal{S} \rightarrow \mathcal{A}$, which is the policy that we are attempting to optimize in the upper-level problem. The upper-level problem takes two “inputs” related to the lower-level problem: (1) J_1 , an approximation

⁴We include time indexing on the value function to emphasize that this Bellman operator is used in a finite-horizon (i.e., non-stationary) setting, but the definition of \tilde{H} itself does not depend on t .

⁵Even in the case that the expectation is approximated via sampling, the former requires sampling from a lower-dimensional successor state distribution.

of the optimal lower-level value J_1^* , (2) $\boldsymbol{\pi}$, a lower-level finite-horizon policy. Fixing these inputs, the value at state $s_0 = (x_0, y_0)$ by executing policy μ is

$$V^\mu(s_0, J_1, \boldsymbol{\pi}) = \mathbb{E}[\tilde{R}(s_0, \mu(s_0), J_1) + \gamma^T V^\mu(s_T(\mu, \boldsymbol{\pi}), J_1, \boldsymbol{\pi})],$$

where $s_T(\mu, \boldsymbol{\pi})$ is the state reached according to the true system dynamics by following $(\mu, \boldsymbol{\pi})$, starting from s_0 and

$$\tilde{R}(s_0, a, J_1) = r(s_0, a) + \gamma J_1(f(s_0, a, w)) \quad (13)$$

is a one-step approximation to the T -period reward function R , defined in (7). Figure 3 helps to visualize the upper-level MDP.

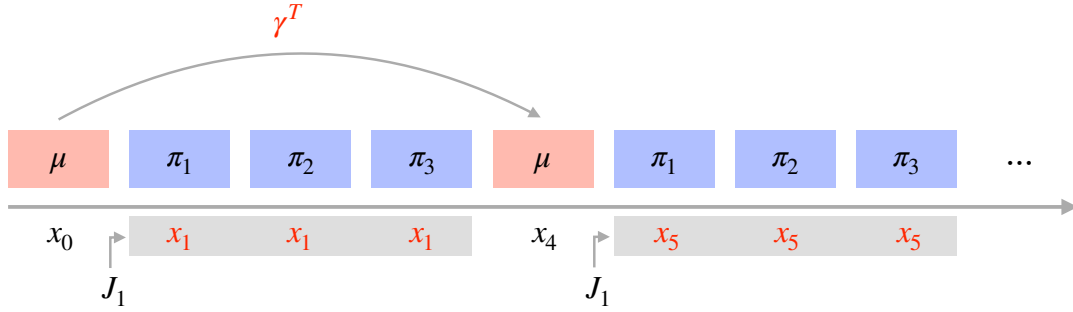


Figure 3: Illustration of the upper-level problem. Notably, the discount factor is γ^T and the reward function, from the point of view of μ , depends on the lower-level value function J_1 . This value function is computed by freezing states, as visualized by the grey box.

The optimal value (for this approximation) at state s_0 can be written as

$$V^*(s_0, J_1, \boldsymbol{\pi}) = \max_a \mathbb{E}[\tilde{R}(s_0, a, J_1) + \gamma^T V^*(s_T(a, \boldsymbol{\pi}), J_1, \boldsymbol{\pi})], \quad (14)$$

where $s_T(a, \boldsymbol{\pi})$ is the state reached according to the true system dynamics by first taking action a and then following $\boldsymbol{\pi}$, starting from s_0 .

Throughout the paper, we use the notation $V^\mu(J_1, \boldsymbol{\pi})$ and $V^*(J_1, \boldsymbol{\pi})$ to refer to the value function (i.e., $\mathcal{S} \rightarrow \mathbb{R}$) obtained when the MDP is evaluated or solved for a fixed J_1 and $\boldsymbol{\pi}$. We also define the Bellman operator associated with (14):

$$(F_{J_1, \boldsymbol{\pi}} V)(s_0) = \max_a \mathbb{E}[\tilde{R}(s_0, a, J_1) + \gamma^T V(s_T(a, \boldsymbol{\pi}))], \quad (15)$$

which will become useful later on.

Recall that the optimal lower-level policy (that solves the frozen-state model) is denoted $\tilde{\pi}^*$ and its optimal value is J_1^* . Let $\tilde{\mu}^*$ be the optimal upper-level policy corresponding to these inputs, i.e., the policy greedy with respect to $V^*(s_0, J_1^*, \tilde{\pi}^*)$. Thus, $(\tilde{\mu}^*, \tilde{\pi}^*)$ is the resulting T -periodic policy from the frozen-state hierarchical approximation; we refer to it as the T -periodic frozen-state policy.

4.3 Characterizing the Exact and Frozen-State Reward Functions

Recall that (μ^*, π^*) is an optimal T -periodic policy of the base model's hierarchical reformulation (8). Suppose π^* is available. Then, the Bellman equation of the base model reformulation is

$$\begin{aligned}
U^*(x_0, y_0) &= \bar{U}^*(x_0, y_0) \\
&= \max_a \mathbb{E} [R(x_0, y_0, a, \pi^*) + \gamma^T \bar{U}^*(x_T, y_T)] \\
&= \max_a \mathbb{E} \left[r(x_0, y_0, a) + \sum_{t=1}^{T-1} \gamma^t r(x_t, y_t, \pi_t^*) + \gamma^T U^*(x_T, y_T) \right] \\
&= \max_a \mathbb{E} \left[r(x_0, y_0, a) + \gamma (H^{T-1} U^*)(x_1, y_1) \right], \tag{16}
\end{aligned}$$

where the notation H^k is shorthand for k applications of the operator H , i.e., $H^k U = H(H^{k-1} U)$ and $H^1 U = HU$. Therefore, the expected T -horizon reward can be written as

$$\mathbb{E} [R(x_0, y_0, a, \pi^*)] = \mathbb{E} \left[r(x_0, y_0, a) + \gamma (H^{T-1} U^*)(x_1, y_1) - \gamma^T U^*(x_T, y_T) \right]. \tag{17}$$

Given the optimal value J_1^* of the lower level (10), the T -horizon reward of the upper level (14) can be written as

$$\begin{aligned}
\mathbb{E} [\tilde{R}(x_0, y_0, a, J_1^*)] &= r(x_0, y_0, a) + \gamma \mathbb{E} [J_1^*(x_1, y_1)] \\
&= r(x_0, y_0, a) + \gamma (\tilde{H}^{T-1} J_T^*)(x_1, y_1), \\
&= r(x_0, y_0, a) + \gamma (\tilde{H}^{T-1} \mathbf{0})(x_1, y_1), \tag{18}
\end{aligned}$$

where $\mathbf{0}$ is the all-zero value function. The difference between (17) and (18) can be interpreted as follows: in the former, we follow a lower-level policy that is *aware* of a terminal value U^* (but

exclude that value when defining the T -horizon reward), while in the latter, we follow a lower-level policy that sees zero terminal reward at the end of the $T - 1$ periods.

The first step to understanding the performance of the frozen-state policy is to analyze the reward approximation $\mathbb{E}[\tilde{R}(s_0, a, J_1^*)]$ compared to the true reward $\mathbb{E}[R(s_0, a, \boldsymbol{\pi}^*)]$. Proposition 4.1 shows how the difference between two reward functions is dependent on the number of frozen periods T , along with the problem parameters.

Proposition 4.1 (Reward Approximation Error). *Let $\langle \mathcal{S}, \mathcal{A}, \mathcal{W}, f, r, \gamma \rangle$ be a $(\alpha, d_{\mathcal{Y}})$ -fast-slow MDP satisfying Assumption 2. Let $\boldsymbol{\pi}^*$ be the optimal lower-level policy for the base model reformulation (8) and J_1^* be the optimal (first-stage) value of the lower-level problem in the frozen-state approximation (10). For any state $s_0 = (x_0, y_0)$ and action a , the approximation error between the T -horizon reward of hierarchical reformulation and the frozen-state approximation, i.e., the discrepancy between (17) and (18), can be bounded as:*

$$\begin{aligned} & \left| \mathbb{E}[R(s_0, a, \boldsymbol{\pi}^*)] - \mathbb{E}[\tilde{R}(s_0, a, J_1^*)] \right| \\ & \leq \alpha d_{\mathcal{Y}} \left(L_r \sum_{i=1}^{T-2} \gamma^i \sum_{j=0}^{i-1} L_f^j \right) + \gamma^{T-1} L_U \left[\alpha d_{\mathcal{Y}} \sum_{j=0}^{T-2} L_f^j + \gamma d_{\mathcal{Y}} (\alpha + 2)(T - 1) \right], \end{aligned} \quad (19)$$

Proof. The detailed proof is in Appendix A.3. □

For more convenient notation, we define $\epsilon_r(\gamma, \alpha, d_{\mathcal{Y}}, L_r, L_f, T)$ to be the right-hand-side of (19):

$$\epsilon_r(\gamma, \alpha, d_{\mathcal{Y}}, \mathbf{L}, T) = \alpha d_{\mathcal{Y}} \left(L_r \sum_{i=1}^{T-2} \gamma^i \sum_{j=0}^{i-1} L_f^j \right) + \gamma^{T-1} L_U \left[\alpha d_{\mathcal{Y}} \sum_{j=0}^{T-2} L_f^j + \gamma d_{\mathcal{Y}} (\alpha + 2)(T - 1) \right],$$

where $\mathbf{L} = (L_r, L_f, L_U)$ emphasizes the dependence on the various Lipschitz constants. In subsequent sections, we use ϵ_r as an ingredient in analyzing the regret of various frozen-state policies.

5 Regret of the Frozen-State Policy $(\tilde{\boldsymbol{\mu}}^*, \tilde{\boldsymbol{\pi}}^*)$

In this section, we will show an upper bound on the regret from applying the T -periodic policy $(\tilde{\boldsymbol{\mu}}^*, \tilde{\boldsymbol{\pi}}^*)$ instead of the optimal policy ν^* in the base model. Note that this is the policy obtained if we were able to perfectly solve the frozen-state approximation. We start with definitions of the

regret of both stationary and T -periodic policies.

Definition 2 (Regret). *Consider a fast-slow MDP with initial state s_0 and optimal policy ν^* . The regret of a stationary policy ν is defined as*

$$\mathcal{R}(s_0, \nu) = U^{\nu^*}(s_0) - U^\nu(s_0) \quad \text{and} \quad \mathcal{R}(\nu) = \max_{s_0} \mathcal{R}(s_0, \nu).$$

The regret of the T -periodic policy $(\mu, \boldsymbol{\pi})$ is defined as:

$$\mathcal{R}(s_0, \mu, \boldsymbol{\pi}) = U^{\nu^*}(s_0) - \bar{U}^\mu(s_0, \boldsymbol{\pi}) = \bar{U}^*(s_0) - \bar{U}^\mu(s_0, \boldsymbol{\pi}) \quad \text{and} \quad \mathcal{R}(\mu, \boldsymbol{\pi}) = \max_{s_0} \mathcal{R}(s_0, \mu, \boldsymbol{\pi}).$$

The second equality in the definition of $\mathcal{R}(s_0, \mu, \boldsymbol{\pi})$ uses the value equivalence between the base model and its hierarchical reformulation (Proposition 3.1).

Remark 3. *As a follow-up comment to Remark 2, notice that $V^*(s_0, J_1^*, \tilde{\boldsymbol{\pi}}^*)$ does not directly enter the regret definition, as $V^*(s_0, J_1^*, \tilde{\boldsymbol{\pi}}^*)$ is just the optimal value of the frozen-state approximation, not the value of its implied greedy policy $\tilde{\mu}^*$ when evaluated in the base model. However, the regret of course depends on $V^*(s_0, J_1^*, \tilde{\boldsymbol{\pi}}^*)$ indirectly, because $\tilde{\mu}^*$ depends on $V^*(s_0, J_1^*, \tilde{\boldsymbol{\pi}}^*)$.*

In this section, we derive a bound on $\mathcal{R}(\tilde{\mu}^*, \tilde{\boldsymbol{\pi}}^*)$, the regret of applying T -periodic policy $(\tilde{\mu}^*, \tilde{\boldsymbol{\pi}}^*)$ to the base model. First, we start with a general lemma, that will be used throughout the paper as a tool to analyze variants of FSVI.

Lemma 5.1. *Suppose we have an approximation $(\boldsymbol{\pi}, J_1)$ to the lower-level solution $(\boldsymbol{\pi}^*, U^*)$. Further, suppose we have an approximation V to the upper-level solution $V^*(J_1, \boldsymbol{\pi})$. Consider a T -periodic policy $(\mu, \boldsymbol{\pi})$, where*

$$\mu(s_0) = \arg \max_{a \in \mathcal{A}} \mathbb{E}[\tilde{R}(s_0, a, J_1) + \gamma^T V(s_T(a, \boldsymbol{\pi}))]. \quad (20)$$

Then, the regret of $(\mu, \boldsymbol{\pi})$ can be bounded as follows:

$$\begin{aligned} \mathcal{R}(\mu, \boldsymbol{\pi}) &\leq \left(\frac{2\gamma^T}{(1-\gamma^T)^2} + \frac{2}{1-\gamma^T} \right) \epsilon_r(\boldsymbol{\pi}^*, J_1) \\ &\quad + \left(\frac{2\gamma^{2T}}{(1-\gamma^T)^2} + \frac{2\gamma^T}{1-\gamma^T} \right) L_U d(\alpha, d_{\mathcal{Y}}, T) + \frac{2\gamma^T}{1-\gamma^T} \|V^*(J_1, \boldsymbol{\pi}) - V\|_\infty, \end{aligned}$$

where $\epsilon_r(\boldsymbol{\pi}^*, J_1) = \max_{s,a} |\mathbb{E}[R(s, a, \boldsymbol{\pi}^*)] - \mathbb{E}[\tilde{R}(s, a, J_1)]|$ and $d(\alpha, d_{\mathcal{Y}}, T) = 2d_{\mathcal{Y}}(\alpha + 1)(T - 1)$.

Proof. See Appendix B.2. □

This result above can be interpreted as the regret being bounded by

$$\text{reward error} + \text{end-of-horizon error} + V\text{-approximation error},$$

which directly corresponds to the three terms in the bound. The reward error is due to freezing the slow state; the end-of-horizon error is due to using zero terminal value; and the V -approximation error is due to not solving the upper-level problem exactly.

The main result of this section follows directly from Lemma 5.1 and is given in Theorem 5.1, which shows the expected regret $\mathcal{R}(\tilde{\boldsymbol{\mu}}^*, \tilde{\boldsymbol{\pi}}^*)$ of applying the policy learned from the frozen-state hierarchical approximation to the base model.

Theorem 5.1. *Let $\langle \mathcal{S}, \mathcal{A}, \mathcal{W}, f, r, \gamma \rangle$ be a $(\alpha, d_{\mathcal{Y}})$ -fast-slow MDP satisfying Assumption 2. The regret of applying the T -periodic policy $(\tilde{\boldsymbol{\mu}}^*, \tilde{\boldsymbol{\pi}}^*)$ in the base model is bounded by*

$$\mathcal{R}(\tilde{\boldsymbol{\mu}}^*, \tilde{\boldsymbol{\pi}}^*) \leq \left(\frac{2\gamma^T}{(1 - \gamma^T)^2} + \frac{2}{1 - \gamma^T} \right) \epsilon_r(\gamma, \alpha, d_{\mathcal{Y}}, \mathbf{L}, T) + \left(\frac{2\gamma^{2T}}{(1 - \gamma^T)^2} + \frac{2\gamma^T}{1 - \gamma^T} \right) L_U d(\alpha, d_{\mathcal{Y}}, T)$$

where $d(\alpha, d_{\mathcal{Y}}, T) = 2d_{\mathcal{Y}}(\alpha + 1)(T - 1)$.

Proof. We apply Lemma 5.1 with $\boldsymbol{\pi} = \tilde{\boldsymbol{\pi}}^*$, $J_1 = J_1^*$, and $V = V^*(J_1^*, \tilde{\boldsymbol{\pi}}^*)$, while noting that by Proposition 4.1, $\epsilon_r(\boldsymbol{\pi}^*, J_1) \leq \epsilon_r(\gamma, \alpha, d_{\mathcal{Y}}, \mathbf{L}, T)$. □

6 Frozen-State Value Iteration

In this section, we introduce the our new approach: the *frozen-state value iteration* (FSVI) algorithm. The main ideas of our approach are:

1. Solve the lower-level MDP with frozen states to obtain a policy $\tilde{\boldsymbol{\pi}}^*$ and its value J_1^* . Since the lower-level problem is a finite horizon MDP, it can be solved exactly using $T - 1$ steps of VI.
2. Apply value iteration (VI) to the upper-level problem starting with some initial value function V^0 , while using J_1^* to approximate the T -horizon reward and $\tilde{\boldsymbol{\pi}}^*$ for T -step transitions. Note

that this is an infinite-horizon MDP that operates at a slower timescale and enjoys a *much more favorable* discount factor of γ^T .

Before we dive into the details and analysis of FSVI, we start by mentioning that the naive approach to solving the base model MDP (5) is to directly apply standard VI (see, e.g., Bertsekas and Tsitsiklis (1996)). For completeness, we provide the full description in Algorithm 1.

Algorithm 1: Exact VI for the Base Model

Input: Initial values U^0 , number of iterations k .
Output: Approximation to the optimal policy ν^k .

```

1 for  $i = 1, 2, \dots, k$  do
2   for  $s$  in the state space  $\mathcal{S}$  do
3      $U^i(s) = \max_a r(s, a) + \gamma \mathbb{E}[U^{i-1}(f(s, a, w))]$ .
4   end
5 end
6 for  $s$  in the state space  $\mathcal{S}$  do
7    $\nu^k(s) = \arg \max_a r(s, a) + \gamma \mathbb{E}[U^k(f(s, a, w))]$ .
8 end

```

Proposition 6.1 is a well-known property that gives the required number of iterations of exact VI on the base model needed for the resulting policy to achieve a desired level of regret.

Proposition 6.1. *Let ν^k be the result of running Algorithm 1 on the base model (5). Then,*

$$\mathcal{R}(\nu^k) = \|U^{\nu^k} - U^*\|_\infty \leq \frac{2r_{\max}\gamma^{k+1}}{(1-\gamma)^2}.$$

Proof. See Appendix C.2. □

6.1 Analysis of FSVI

A detailed specification is given in Algorithm 2. We denote the resulting value function approximation after k iterations of value iteration as V^k , from which we obtain a policy $\tilde{\mu}^k$. The T -periodic policy output by FSVI is formed by combining $\tilde{\mu}^k$ with the optimal finite-horizon policy $\tilde{\pi}^*$ from the lower-level MDP: $(\tilde{\mu}^k, \tilde{\pi}^*)$.

Algorithm 2: Frozen-State Value Iteration (FSVI)

Input: Initial values $J_T^* \equiv 0$ and V^0 , number of iterations k .

Output: Approximation of the T -periodic frozen-state policy $(\tilde{\mu}^k, \tilde{\pi}^*)$ and J_1^* .

```
1 for  $t = T - 1, T - 2, \dots, 1$  do
2   | for each slow state  $x \in \mathcal{X}$  do
3   |   | for each fast state  $y \in \mathcal{Y}$  do
4   |   |   |  $J_t^*(x, y) = \max_a r(x, y, a) + \gamma \mathbb{E}[J_{t+1}^*(x, f_{\mathcal{Y}}(x, y, a, w))]$ .
5   |   |   |  $\tilde{\pi}_t^*(x, y) = \arg \max_a r(x, y, a) + \gamma \mathbb{E}[J_{t+1}^*(x, f_{\mathcal{Y}}(x, y, a, w))]$ .
6   |   |   | end
7   |   |   | end
8   |   |   | end
9   |   |   | end
10  |   |   | end
11  |   |   |  $V^i(x_0, y_0, J_1^*, \tilde{\pi}^*) = \max_a \mathbb{E}[\tilde{R}(s_0, a, J_1^*) + \gamma^T V^{i-1}(x_T, y_T, J_1^*, \tilde{\pi}^*)]$ .
12  |   |   | end
13  |   |   | end
14  |   |   | end
15  |   |   |  $\tilde{\mu}^k(x_0, y_0) = \arg \max_a \mathbb{E}[\tilde{R}(s_0, a, J_1^*) + \gamma^T V^k(x_T, y_T, J_1^*, \tilde{\pi}^*)]$ .
16  |   |   | end
```

An instance of FSVI is associated with two primary quantities: k , the number of VI iterations, and T , the number of periods the slow state is frozen in the frozen-state approximation. The next theorem makes use of this lemma to provide a bound on the regret of the policy obtained for a particular k and T .

Theorem 6.1. *Let $(\tilde{\mu}^k, \tilde{\pi}^*)$ be the resulting T -periodic policy after running FSVI for k iterations. The regret incurred when running $(\tilde{\mu}^k, \tilde{\pi}^*)$ in the base model satisfies*

$$\begin{aligned} \mathcal{R}(\tilde{\mu}^k, \tilde{\pi}^*) \leq & \left(\frac{2\gamma^T}{(1-\gamma^T)^2} + \frac{2}{1-\gamma^T} \right) \epsilon_r(\gamma, \alpha, d_{\mathcal{Y}}, \mathbf{L}, T) \\ & + \left(\frac{2\gamma^{2T}}{(1-\gamma^T)^2} + \frac{2\gamma^T}{1-\gamma^T} \right) L_U d(\alpha, d_{\mathcal{Y}}, T) + \frac{2r_{\max}\gamma^{(k+1)T}}{(1-\gamma)(1-\gamma^T)}, \end{aligned}$$

where the last term, which depends on k , accounts for the error due to value iteration.

Proof. See Appendix C.3. □

6.2 Running Time of FSVI

It is well-known that each iteration of standard VI has time complexity $\mathcal{O}(|\mathcal{S}|^2|\mathcal{A}|)$, which provides a contraction factor of γ (Littman et al., 1995). The upper level of FSVI, on the other hand, enjoys an improved contraction factor γ^T with the same per-iteration running time of $\mathcal{O}(|\mathcal{S}|^2|\mathcal{A}|)$, given that we pay a *one-time fixed cost* of solving the lower level. The $\mathcal{O}(|\mathcal{S}|^2|\mathcal{A}|)$ consists of $|\mathcal{S}||\mathcal{A}|$ due to the number of state-action pairs at which to compute the Bellman update and another factor of $|\mathcal{S}|$ due to the number of successor states. Since freezing slow states restricts the successor states to \mathcal{Y} , each iteration of the lower-level VI (Lines 2-7 of Algorithm 2) has running time $\mathcal{O}(|\mathcal{X}||\mathcal{Y}|^2|\mathcal{A}|)$. An additional $\mathcal{O}(|\mathcal{S}|^2 T)$ is required to compute the T -step transition probabilities of following $\tilde{\pi}^*$, to be used in the upper-level VI, resulting in a one-time fixed cost of $\mathcal{O}(|\mathcal{X}||\mathcal{Y}|^2|\mathcal{A}| T + |\mathcal{S}|^2 T)$. Particularly when $|\mathcal{X}|$ is large, this can be a reasonable fixed cost to pay in order to get the much improved discount factor of γ^T going forward (as we will show in the numerical results of Section 9). In Sections 7 and 8, we propose two extensions to FSVI that further reduce its computational requirements.

7 An Approximation for Nearly-Factored MDPs

One potential drawback of Algorithm 2 is that solving the lower-level problem requires solving an MDP for each slow state $x \in \mathcal{X}$. In this section, we consider the situation where the reward function satisfies a certain *nearly-factored* assumption. In such a case, it is possible to design an extension of FSVI that solves the lower-level problem for a *nominal* slow state (or a small number of slow states) and then leverage the nearly-factored structure to approximate the lower-level values at other slow states. Such a scheme would lower the one-time, fixed computational cost (i.e., the effort required to solve the lower-level problem) of applying FSVI.

Assumption 3 (Nearly-Factored Reward). *A fast-slow MDP $\langle \mathcal{S}, \mathcal{A}, \mathcal{W}, f, r, \gamma \rangle$ has a “nearly-factored” reward if there exists functions g , h , and $\zeta > 0$ such that:*

$$|g(x) + h(y, a) - r(x, y, a)| \leq \zeta, \quad \text{for all } x \in \mathcal{X}, y \in \mathcal{Y}, a \in \mathcal{A}.$$

In other words, the reward r is a sum of slow and fast components with error at most ζ .

This terminology comes from the notion *factored* MDPs, a commonly-studied type of weakly-connected structure that notably assumes an additive reward function (see, e.g., [Boutillier et al. \(2000\)](#) and [Osband and Van Roy \(2014\)](#)). Although the analysis in this paper is based on additive separability of the reward function (i.e., $r(x, y, a) \approx g(x) + h(y, a)$), it is easy to extend the analysis to other types of separable rewards, such as $r(x, y, a) \approx \langle g(x), h(y, a) \rangle$.

7.1 The Nominal-State Approximation in the Lower Level

We now seek to reduce the amount of computation needed to solve the lower-level MDP in the case where Assumption 3 holds. The two main ingredients of our approach are:

1. An approximation the lower-level (frozen-state) MDP by another MDP with reward function exactly equal to $g(x) + h(y, a)$, instead of $r(s, a)$. We call it the *separable approximation* of the lower-level MDP.
2. A solution $\bar{J}_1(x^*, y)$ to the separable approximation at a particular *nominal state*⁶ $x^* \in \mathcal{X}$.

⁶In this section, we discuss the case with a single nominal slow state x^* for simplicity. An extension to multiple

For any other $x \in \mathcal{X}$, we can use Assumption 3 as a basis to approximate the value at x using only $\bar{J}_1(x^*, y)$, without the need to solve an MDP for slow state x .

Fix a nominal state $x^* \in \mathcal{X}$. The Bellman recursion for the separable approximation at x^* is analogous to (10): let $\bar{J}_T \equiv 0$ and for $t = 1, 2, \dots, T-1$, let

$$\bar{J}_t(x^*, y) = \max_a g(x^*) + h(y, a) + \gamma \mathbb{E}[\bar{J}_{t+1}(x^*, y')], \quad (21)$$

where $y' = f_{\mathcal{Y}}(x^*, y, a, w)$. Note that x^* continues to be frozen and we have simply replaced the reward r with $g + h$. Let $\bar{\pi}$ be $(T-1)$ -period policy associated with (21). Since \bar{J}_t is only defined for the slow state x^* , we need to extend it to $x \neq x^*$. Let $\Delta_g(x) = g(x) - g(x^*)$. Leveraging the separability of the reward function, we propose

$$\bar{J}_t(x, y) = \sum_{i=0}^{T-t-1} \gamma^i \Delta_g(x) + \bar{J}_t(x^*, y), \quad (22)$$

where we account for the reward error by applying a correction (but we do not account for error in the transitions from using x^* instead of x ; see Lemma 7.1 for a full analysis). Such an approximation allows for solving the frozen-state MDP only for x^* and using the result to approximate the value for other slow states, dramatically reducing the amount of overhead when using FSVI. The Nominal FSVI algorithm makes use of this idea and is introduced in Algorithm 3.

Lemma 7.1. *Consider $\bar{J}_t(x, y)$, as defined by (21) and (22), which is an approximation to the true frozen-state value $J_t^*(x, y)$, as defined in (10). Under Assumption 3, it holds that:*

$$\begin{aligned} |\bar{J}_t(x, y) - J_t^*(\tilde{x}, \tilde{y})| &\leq \left(\sum_{i=0}^{T-t-1} \gamma^i \right) (\zeta + L_r \|x - \tilde{x}\|_2) + \left(\sum_{i=0}^{T-t-1} \gamma^i L_f^i \right) L_r \|y - \tilde{y}\|_2 \\ &\quad + \left(\sum_{i=1}^{T-t-1} L_f^i \sum_{j=i}^{T-t-1} \gamma^j \right) L_r \|x^* - \tilde{x}\|_2. \end{aligned}$$

Proof. See Appendix D.1. □

The next proposition is a simple consequence of Lemma 7.1.

nominal slow states is straightforward.

Algorithm 3: Nominal FSVI

Input: A nominal state x^* , initial values $\bar{J}_T \equiv 0$ and V^0 , number of iterations k .

Output: Approximation of the T -periodic frozen-state policy $(\bar{\mu}_{\text{nom}}^k, \bar{\pi}_{\text{nom}})$ and \bar{J}_1 .

```

1 for  $t = T - 1, T - 2, \dots, 1$  do
2   for each fast state  $y \in \mathcal{Y}$  do
3      $\bar{J}_t(x^*, y) = \max_a g(x^*) + h(y, a) + \gamma \mathbb{E}[\bar{J}_{t+1}(x^*, f_{\mathcal{Y}}(x^*, y, a, w))]$ .
4   end
5 end
6 Define  $\bar{J}_t(x, y)$  using (22) and let  $\bar{\pi}_{\text{nom}}$  be greedy with respect to  $\bar{J}_t$ .
7 for  $i = 1, 2, \dots, k$  do
8   for  $s_0 = (x_0, y_0)$  in the state space  $\mathcal{X} \times \mathcal{Y}$  do
9      $V^i(x_0, y_0, \bar{J}_1, \bar{\pi}_{\text{nom}}) = \max_a \mathbb{E}[\tilde{R}(s_0, a, \bar{J}_1) + \gamma^T V^{i-1}(x_T, y_T, \bar{J}_1, \bar{\pi}_{\text{nom}})]$ .
10  end
11 end
12 for  $s_0 = (x_0, y_0)$  in the state space  $\mathcal{X} \times \mathcal{Y}$  do
13    $\bar{\mu}_{\text{nom}}^k(x_0, y_0) = \arg \max_a \mathbb{E}[\tilde{R}(s_0, a, \bar{J}_1) + \gamma^T V^k(x_T, y_T, \bar{J}_1, \bar{\pi}_{\text{nom}})]$ .
14 end

```

Proposition 7.1. Recall from (13) the definition of $\tilde{R}(s_0, a, J_1)$, the approximation of the T -period reward function. Under Assumption 3, the error between using a nominal state approximation versus fully optimizing the frozen-state lower level is:

$$|\mathbb{E}[\tilde{R}(s_0, a, J_1^*)] - \mathbb{E}[\tilde{R}(s_0, a, \bar{J}_1)]| \leq \sum_{i=1}^{T-1} \gamma^i \zeta + \left(\sum_{i=1}^{T-2} L_f^i \sum_{j=i+1}^{T-1} \gamma^j \right) L_r \max_x \|x^* - x\|_2,$$

where J_t^* is computed as in Algorithm 2 and \bar{J}_t is computed as in Algorithm 3.

Proof. See Appendix D.2. □

Theorem 7.1. Let $(\bar{\mu}_{\text{nom}}^k, \bar{\pi}_{\text{nom}})$ be the result after running Nominal FSVI for k iterations with nominal state x^* . The regret incurred when running $(\bar{\mu}_{\text{nom}}^k, \bar{\pi}_{\text{nom}})$ in the base model satisfies

$$\begin{aligned} \mathcal{R}(\bar{\mu}_{\text{nom}}^k, \bar{\pi}_{\text{nom}}) &\leq \left(\frac{2\gamma^T}{(1-\gamma^T)^2} + \frac{2}{1-\gamma^T} \right) \epsilon_{r,\text{nom}}(\gamma, \alpha, d_{\mathcal{Y}}, \mathbf{L}, T, \zeta, x^*) \\ &\quad + \left(\frac{2\gamma^{2T}}{(1-\gamma^T)^2} + \frac{2\gamma^T}{1-\gamma^T} \right) L_U d(\alpha, d_{\mathcal{Y}}, T) + \frac{2r_{\max}\gamma^{(k+1)T}}{(1-\gamma)(1-\gamma^T)}, \end{aligned}$$

where the reward error is given by

$$\begin{aligned} \epsilon_{r,\text{nom}}(\gamma, \alpha, d_{\mathcal{Y}}, \mathbf{L}, T, \zeta, x^*) \\ = \epsilon_r(\gamma, \alpha, d_{\mathcal{Y}}, \mathbf{L}, T) + \sum_{i=1}^{T-1} \gamma^i \zeta + \left(\sum_{i=1}^{T-2} L_f^i \sum_{j=i+1}^{T-1} \gamma^j \right) L_r \max_x \|x^* - x\|_2. \end{aligned}$$

Proof. The proof is similar to the proof of Theorem 5.1, except we need to compute the $\epsilon_r(\boldsymbol{\pi}^*, \bar{J}_1)$ term of Lemma 5.1. Combining Proposition 7.1 with the result in Proposition 4.1, we can see that $\epsilon_{r,\text{nom}}(\gamma, \alpha, d_{\mathcal{Y}}, \mathbf{L}, T, \zeta, x^*)$ bounds $\epsilon_r(\boldsymbol{\pi}^*, \bar{J}_1)$. \square

8 Value Function Approximation with a Linear Architecture

So far in this paper, we have proposed a frozen-state approximation that is able to exploit a certain fast-slow problem structure. We then proposed another level of approximation using nominal slow states, which is valid when the MDP has a nearly-factored reward function. Both of these approximations use a tabular value function representation and therefore, each iteration of VI in the upper level requires looping through the entire state space $\mathcal{X} \times \mathcal{Y}$ (although the nominal-state approximation does reduce the computational burden in the lower-level problem).

In this section, we explore the use of a linear architecture for a more compact representation of the value function. We show how *approximate* VI (AVI) can be combined with the frozen-state approximation, resulting in an algorithm that can scale to fast-slow MDPs with much larger state spaces. The form of AVI that we use is based on the technique first proposed in Tsitsiklis and Van Roy (1996) and later also used in Zanette et al. (2019). A technical contribution we make here is to prove error bounds when this approximation architecture is used in a hierarchical setting that combines finite-horizon and infinite-horizon components (i.e., our frozen-state VI).

8.1 The Approximation Architecture

Let $\phi(s) = (\phi_1(s), \phi_2(s), \dots, \phi_M(s))^T \in \mathbb{R}^M$ be an M -dimensional feature vector evaluated at state $s \in \mathcal{S}$. An approximation $\{\hat{J}_t(\boldsymbol{\omega}_t)\}_{t=1}^T$ of the lower-level value functions $\{J_t^*\}_{t=1}^T$ of the frozen-state approximation is given by a sequence of parameter vectors $\{\boldsymbol{\omega}_t\}_{t=1}^T$ with $\boldsymbol{\omega}_t \in \mathbb{R}^M$, where the

component of $\hat{J}_t(\boldsymbol{\omega}_t)$ associated with s is given by

$$\hat{J}_t(s, \boldsymbol{\omega}_t) = \boldsymbol{\phi}^\top(s) \boldsymbol{\omega}_t, \quad \text{for } t = 1, 2, \dots, T.$$

(Note that since $J_T^* \equiv 0$, we can set $\boldsymbol{\omega}_T = \mathbf{0}$.) The approximation $\hat{V}(\boldsymbol{\beta})$ to the upper-level value function (of the frozen-state model) $V^*(J_1^*, \tilde{\boldsymbol{\pi}}^*)$ is given by a parameter vector $\boldsymbol{\beta} \in \mathbb{R}^M$, where

$$\hat{V}(s, \boldsymbol{\beta}) = \boldsymbol{\phi}^\top(s) \boldsymbol{\beta}.$$

For simplicity, we have used the same features in both the upper and lower levels.

It is well-known that naive specifications of approximate value iteration applied to linear architectures can produce divergent behavior (Bertsekas and Tsitsiklis, 1996). To circumvent this potential issue, our algorithmic approach depends on a set of *pre-selected* states $\tilde{\mathcal{S}} = \{s_1, s_2, \dots, s_M\}$, an idea popularized in Tsitsiklis and Van Roy (1996), who showed that if certain assumptions on these states and the feature vectors are satisfied, then divergence is avoided. A similar algorithm is also described more recently in Zanette et al. (2019).

In this section, we need an ordering of the state space, so without loss of generality, we assume that $\mathcal{S} = \{1, 2, \dots, N\}$ and that the first M are the pre-selected states, i.e., $s_m = m$ for $m = 1, 2, \dots, M$. We make the following assumption on the feature vectors; this is essentially Assumption 2 of Tsitsiklis and Van Roy (1996), adapted to our setting.

Assumption 4. *Let $\tilde{\mathcal{S}} = \{s_1, s_2, \dots, s_M\}$ be a set of pre-selected anchor states. Suppose the following conditions on the features $\boldsymbol{\phi}$ are satisfied.*

1. *The vectors $\boldsymbol{\phi}(s_1), \boldsymbol{\phi}(s_2), \dots, \boldsymbol{\phi}(s_M)$ are linearly independent.*
2. *There exists some $\gamma' \in [\gamma, 1)$ such that for any state $s \in \mathcal{S}$, there are coefficients $\theta_m(s) \in \mathbb{R}$ for $m = 1, 2, \dots, M$ satisfying:*

$$\sum_{m=1}^M |\theta_m(s)| \leq 1 \quad \text{and} \quad \boldsymbol{\phi}(s) = \frac{\gamma'}{\gamma} \sum_{m=1}^M \theta_m(s) \boldsymbol{\phi}(s_m).$$

The interpretation of this assumption is that the feature space $\{\boldsymbol{\phi}(s) \mid s \in \mathcal{S}\}$ lies in the convex hull

of the points defined by the pre-selected states: $\{\pm(\gamma'/\gamma)\phi(s_m)\}_{m=1}^M$. To reduce notional clutter, we will define $\kappa = \gamma'/\gamma$ to be the amplification factor induced by the features.

Following [Tsitsiklis and Van Roy \(1996\)](#), we let $\Phi \in \mathbb{R}^{N \times M}$ be a matrix with the s -th row equal to $\phi^\top(s)$ and let $L \in \mathbb{R}^{M \times M}$ be a matrix with the m -th row equal to $\phi^\top(s_m)$. If we let G be the remaining rows of Φ , then we see that $\Phi = [L; G]$. Next, by Assumption 4, the matrix L has a unique matrix inverse $L^{-1} \in \mathbb{R}^{M \times M}$. We define $\Phi^\dagger \in \mathbb{R}^{M \times N}$ as follows: for $m \in \{1, 2, \dots, M\}$, suppose the m -th column of Φ^\dagger is equal to the m -th column of L^{-1} , and let all the other entries of Φ^\dagger be zero. In other words, $\Phi^\dagger = [L^{-1} \ 0]$. Therefore, we see that Φ^\dagger is a left inverse of Φ :

$$\Phi^\dagger \Phi = [L^{-1} \ 0] \begin{bmatrix} L \\ G \end{bmatrix} = L^{-1}L = \mathbf{I},$$

where $\mathbf{I} \in \mathbb{R}^{M \times M}$ is the identity matrix.

8.2 Frozen-State Approximate Value Iteration

Recall the lower-level Bellman operator \bar{H} from (12) and the upper-level Bellman operator $F_{\hat{J}_1, \hat{\pi}}$ defined in (15). The high-level idea behind our new approach, *frozen-state approximate value iteration* (FSAVI) is as follows:

- **Lower-level AVI.** We first run approximate value iteration (under basis functions Φ) for the lower-level problem. Letting $\omega_T^* = \mathbf{0}$, the parameter ω_t^* is estimated by first evaluating $\bar{H}\hat{J}_{t+1}(\omega_{t+1}^*)$ at the pre-selected states, and then computing ω_t^* so that $\hat{J}_t(s, \omega_t^*) = (\bar{H}\hat{J}_{t+1}(\omega_{t+1}^*))(s)$ for $s \in \tilde{\mathcal{S}}$.
- **Upper-level AVI.** Suppose that after solving the lower level, we have parameter vectors $\omega^* = (\omega_1^*, \omega_2^*, \dots, \omega_T^*)$, implying lower-level value functions $\hat{J}_t(\omega_t^*) = \Phi \omega_t^*$ and an associated greedy policy $\hat{\pi}(\omega^*) = (\hat{\pi}_1(\omega^*), \dots, \hat{\pi}_{T-1}(\omega^*))$:

$$\hat{\pi}_t(x, y, \omega^*) = \arg \max_a r(x, y, a) + \gamma \mathbb{E}[\hat{J}_{t+1}(x, y', \omega_{t+1}^*)]. \quad (23)$$

For the upper level, the parameter β_k is updated to β_{k+1} in iteration $k+1$ by first evaluating $F_{\hat{J}_1(\omega_1^*), \hat{\pi}(\omega^*)}\hat{V}(\beta_k)$ at the pre-selected states, then computing β_{k+1} so that $\hat{V}(s, \beta_{k+1}) =$

$(F_{\hat{J}_1(\omega_1^*), \hat{\pi}(\omega^*)} \hat{V}(\beta_k))(s)$ for $s \in \tilde{\mathcal{S}}$. Note that, taking Φ as fixed, the dependence of the upper level on the lower level can be represented succinctly through ω^* . Therefore, we will use the simplified notation $F_\omega := F_{\hat{J}_1(\omega_1), \hat{\pi}(\omega)}$ going forward.

To start, we define two new Bellman operators for the parameter space:

$$\bar{H}' = \Phi^\dagger \circ \bar{H} \circ \Phi \quad \text{and} \quad F'_\omega = \Phi^\dagger \circ F_\omega \circ \Phi.$$

To understand the definition of H' , consider the lower level. Suppose we start with a parameter vector ω_{t+1}^* , representing an approximate value function at time period $t+1$ given by $\hat{J}_{t+1}(\omega_{t+1}^*) = \Phi \omega_{t+1}^*$. The update to the next parameter vector ω_t^* is obtained by applying \bar{H} to $\hat{J}_{t+1}(\omega_{t+1}^*)$, as we would normally do, and then applying Φ^\dagger to project back to the parameter space. For the upper level, a similar logic holds to go from β_i to β_{i+1} : we first have the approximate upper-level value function $\hat{V}(\beta_i) = \Phi \beta_i$ and then apply the normal Bellman update F_{ω^*} , before lastly obtaining the updated parameter β_{i+1} using Φ^\dagger . Therefore, we have

$$\omega_t^* = \bar{H}'(\omega_{t+1}^*) \quad \text{and} \quad \beta_{i+1} = F'_{\omega^*}(\beta_i).$$

We show in the Lemma E.5 of the Appendix that F'_{ω^*} is an $(\kappa\gamma^T)$ -contraction in the norm $\|\cdot\|_\Phi$ on \mathbb{R}^M defined by $\|\beta\|_\Phi = \|\Phi\beta\|_\infty$ and therefore has a fixed point β^* . We now define two quantities related to the approximation error of the linear architecture.

Definition 3. *Define the linear architecture approximation error for the lower level as*

$$\varepsilon_{\text{low}} = \max_{t \in \{1, 2, \dots, T\}} \inf_{\omega_t \in \mathbb{R}^M} \|J_t^* - \hat{J}_t(\omega_t)\|_\infty. \quad (24)$$

Let V_ω^* be the fixed point of F_ω . For the upper level, we define error ε_{up} as

$$\varepsilon_{\text{up}} = \sup_{\omega} \inf_{\beta \in \mathbb{R}^M} \|V_\omega^* - \hat{V}(\beta)\|_\infty. \quad (25)$$

Both (24) and (25) are related to the approximation errors defined in [Tsitsiklis and Van Roy \(1996\)](#); moreover, taking a uniform bound over quantities that need to be approximated resembles the errors defined in [Munos and Szepesvári \(2008\)](#).

Algorithm 4: Frozen-State Approximate Value Iteration (FSAVI)

Input: $\tilde{\mathcal{S}} = \{s_1, s_2, \dots, s_M\}$, ϕ , initial weights $\omega_T = \beta_0 = \mathbf{0}$, number of iterations k .

Output: Approximation of the T -periodic frozen-state policy $(\hat{\mu}_{(\beta^k, \omega^*)}, \hat{\pi}_{\omega^*})$ and $\hat{J}_1(\omega^*)$

```

1 for  $t = T - 1, T - 2, \dots, 1$  do
2   for each pre-selected state  $s = (x, y) \in \tilde{\mathcal{S}}$  do
3      $J_t(x, y) = \max_a r(x, y, a) + \gamma \mathbb{E}[\hat{J}_{t+1}(x, f_{\mathcal{Y}}(x, y, a, w), \omega_{t+1})]$ .
4   end
5   Set remaining entries of  $J_t$  to zero. Update parameter vector:  $\omega_t^* = \Phi^\dagger J_t$ .
6 end
7 Let  $\hat{\pi}_{\omega^*}$  be greedy with respect to  $\hat{J}_t(\omega_t^*) = \Phi \omega_t^*$ , similar to (23).
8 for  $i = 1, 2, \dots, k$  do
9   for each pre-selected state  $s_0 \in \tilde{\mathcal{S}}$  do
10     $V^i(s_0) = \max_a \mathbb{E}[\tilde{R}(s, a, \hat{J}_1(\omega_1^*)) + \gamma^T \hat{V}(s_T(a, \tilde{\pi}_{\text{avi}}), \beta_{i-1})]$ .
11    Set remaining entries of  $V^i$  to zero. Update parameter vector:  $\beta_i = \Phi^\dagger V^i$ .
12  end
13 end
14 for  $s_0$  in the state space  $\mathcal{S}$  do
15   $\hat{\mu}_{(\beta^k, \omega^*)}(s_0) = \arg \max_a \mathbb{E}[\tilde{R}(s_0, a, \hat{J}_1(\omega_1^*)) + \gamma^T \hat{V}(s_T(a, \tilde{\pi}_{\omega^*}), \beta_k)]$ .
16 end

```

Theorem 8.1. Let $(\hat{\mu}_{(\beta^k, \omega^*)}, \hat{\pi}_{\omega^*})$ be the result after running FSAVI for k iterations for a given $\tilde{\mathcal{S}}$ and ϕ . The regret incurred when running $(\hat{\mu}_{(\beta^k, \omega^*)}, \hat{\pi}_{\omega^*})$ in the base model satisfies

$$\begin{aligned} \mathcal{R}(\hat{\mu}_{(\beta^k, \omega^*)}, \hat{\pi}_{\omega^*}) &\leq \left(\frac{2\gamma^T}{(1-\gamma^T)^2} + \frac{2}{1-\gamma^T} \right) \epsilon_{r,\text{avi}}(\gamma, \alpha, d_{\mathcal{Y}}, \mathbf{L}, T, \gamma', \epsilon_{\text{low}}) \\ &+ \left(\frac{2\gamma^{2T}}{(1-\gamma^T)^2} + \frac{2\gamma^T}{1-\gamma^T} \right) L_U d(\alpha, d_{\mathcal{Y}}, T) + \left(\frac{1+\kappa}{1-\kappa\gamma^T} \right) \epsilon_{\text{up}} + (\kappa\gamma^T)^k \left(\frac{\kappa^2 - \kappa^2(\kappa\gamma)^{T+1}}{(1-\kappa\gamma^T)(1-\kappa\gamma)} \right) r_{\text{max}}, \end{aligned}$$

where the reward error is given by

$$\epsilon_{r,\text{avi}}(\gamma, \alpha, d_{\mathcal{Y}}, \mathbf{L}, T, \gamma', \epsilon_{\text{low}}) = \epsilon_r(\gamma, \alpha, d_{\mathcal{Y}}, \mathbf{L}, T) + \left(\frac{1+\kappa}{1-\kappa\gamma} - \frac{(\kappa\gamma)^T(1+\gamma)}{\gamma - \kappa\gamma^2} \right) \epsilon_{\text{low}}.$$

Proof. See Appendix E.2. □

9 Numerical Experiments

We now apply our algorithms to three applied examples: (1) dynamic service allocation for a multi-class queue, (2) restless multi-armed bandit for asset maintenance optimization, and (3) energy demand response. For the service allocation and asset maintenance problems, which have relatively smaller state spaces, we compare the VI-based variants: Base VI, Slow-agnostic VI, Q-learning, FSVI, and Nominal FSVI. For the energy demand response problem, which has a relatively larger state space, we compare the feature-based variants: Base AVI, Slow-agnostic AVI, DQN, FSAVI, and Nominal FSAVI. We study the performance of each method with respect to its running time. Building off of the discussion in Section 6.2, we define the running time of each iteration of a given method to be $|\mathcal{S}_{\text{obs}}||\mathcal{A}||\mathcal{S}_{\text{succ}}|$, where \mathcal{S}_{obs} is the set of states at which we compute the Bellman update and $\mathcal{S}_{\text{succ}}$ is the set of successor states evaluated. We now give more details about the methods being compared.

- Base VI/AVI.** We refer to Algorithm 1 as the “Base VI” approach, which is simply standard VI applied to the base model with no changes (with discount factor γ). The “Base AVI” baseline uses the VI with the linear architecture described in Section 8 directly on the base model. More precisely, it iterates the approximate Bellman operator $\Phi^\dagger \circ H \circ \Phi$, where H is the Bellman operator for the base model defined in (6). For succinctness, we have omitted a detailed algorithm specification. For Base VI, we use exact transition probabilities when computing the expectation in the Bellman update. However, because Base AVI is used for problems with larger state spaces, exact evaluation of the expectation is more difficult. Instead, we resort to using a Monte Carlo-based sample average, with a sample of $|\mathcal{S}_{\text{succ}}| = 40$ successor states.
- Slow-agnostic VI/AVI.** As we discussed in the introduction, simplified decision models that *ignore* the slow state are often used in practice to improve tractability. To make this precise, we propose the following *slow-agnostic* Bellman operator to test a particular instantiation of this idea that averages over slow states and ignores it thereafter:

$$(H_{\text{fast}}W)(y) = \max_{a \in \mathcal{A}} |\mathcal{X}|^{-1} \sum_{x \in \mathcal{X}} \left(r(x, y, a) + \gamma \mathbb{E}[W(f_{\mathcal{Y}}(x, y, a, w))] \right),$$

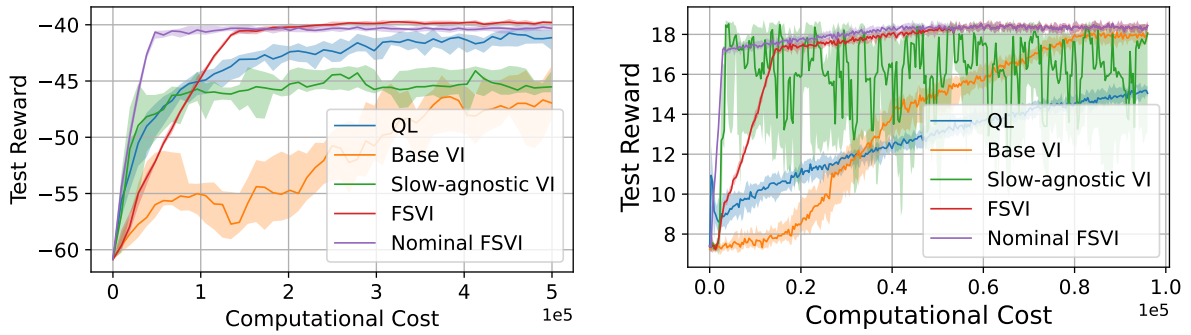
where W is a value function defined only over $y \in \mathcal{Y}$. “Slow-agnostic VI” iterates the operator H_{fast} , while “Slow-agnostic AVI” iterates $\Phi^\dagger \circ H_{\text{fast}} \circ \Phi$. For the AVI version, we use $|\mathcal{S}_{\text{succ}}| = 20$ successor state samples to approximate the expectation (this is smaller than in Base AVI because we only need to sample over \mathcal{Y} , rather than $\mathcal{X} \times \mathcal{Y}$). Upon implementation, the policy ignores the slow state and only uses the value of y to take actions.

- **Q-learning/Deep Q-networks.** We also compare our approaches to the well-known reinforcement learning method, Q-learning (QL) (Watkins, 1989), along with its deep reinforcement learning variant, Deep Q-networks (DQN) (Mnih et al., 2013, 2015).
- **Ours: FSVI/Nominal FSVI (multiple).** Next, we have our VI-based approaches based on the frozen-state approximation. The FSVI and Nominal FSVI methods are described in detail in Algorithms 2 and 3. “Nominal FSVI (multiple)” refers to an extension to multiple nominal states (as mentioned in Section 7). The extension uses 9 nominal states for the service allocation problem (3 in each dimension of the 2-dimensional slow state) and 5 nominal states for the other two problems. The nominal states are equally spaced within the bounds of each slow state dimension. To apply Line 6 of Algorithm 3 (Nominal FSVI), we select the nearest nominal state by Euclidean distance to (x, y) . For both methods, we freeze slow states for $T = 10$ periods.
- **Ours: FSAVI/Nominal FSAVI (multiple)** Lastly, we have our AVI-based frozen-state methods, which also freeze slow states for $T = 10$ periods. FSAVI is described in Algorithm 4 and Nominal FSAVI (multiple) is the natural combination of Nominal FSVI (multiple) and FSAVI; the computational benefit here is that since x^* is fixed, the lower-level linear approximation only needs to be performed over y rather than (x, y) . For both AVI methods, we use $M = 0.3|\mathcal{S}|$ pre-selected states with Gaussian radial basis functions for ϕ .⁷ We use $|\mathcal{S}_{\text{succ}}| = 250$ successor state samples to approximate the expectation, spread over 25 simulated sample paths of the lower-level policy of length $T = 10$.⁸

⁷The M basis functions operate on normalized state space (with each state variable normalized to $[0, 1]$), with their centers spaced evenly and width equal to 0.02.

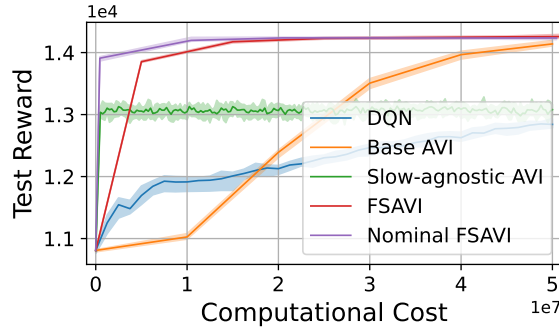
⁸Note that each iteration of the upper level of FSAVI is more computationally intensive than the upper level of Base AVI due to the need for simulating the lower level policy. We account for this accurately in the computational cost calculation to provide a fair comparison.

To evaluate policies, we use a truncated horizon of 100 periods ($10T$) and each method is evaluated over 10 independent runs. In order to create a more fine-grained performance plot, in each Bellman update of the VI-based variants, we allow evaluating the performance of policies “in between” complete iterations of VI, when the Bellman updates have only been executed for a subset of states in the state space. For each run, the order of state updates is randomly shuffled. The AVI-based variants, however, require all pre-selected states to be observed before the parameter vector can be updated; hence, we plot the performance of the policy after each full AVI iteration is complete.



(a) Multi-class service allocation

(b) Restless two-armed bandit



(c) Energy demand response

Figure 4: Performance of each algorithm on the three example applications: (a) multi-class service allocation and queueing, (b) restless two-armed bandit for asset maintenance optimization, and (c) energy demand response. The solid lines show median performance and the error bars represent the 10th-90th percentiles across 10 random seeds. The x -axis shows the computational cost, defined by $|\mathcal{S}_{\text{obs}}||\mathcal{A}||\mathcal{S}_{\text{succ}}|$.

9.1 Multi-Class Service Allocation with Stochastic Holding Costs

We study a version of the multi-class service system problem based on the model presented in Ansell et al. (2003) and later Brown and Haugh (2017), extended to the case of *stochastic holding*

costs. Many variations of the original problem (without stochastic costs) have been studied in the literature; to name a few, see [Cox et al. \(1961\)](#), [Harrison \(1975\)](#), [Van Mieghem \(1995\)](#), and [Gittins \(1979\)](#). Our variant with stochastic holding costs is partially motivated by the model in [Lee and Vojnovic \(2021\)](#), which proposes a learning algorithm for job scheduling. The main idea behind this example is that when the holding cost stochastic process evolves slowly, it becomes a reasonable candidate for the slow state in our frozen-state framework.

We consider a single server and two classes of customers. For class $j \in \{1, 2\}$, the arrival rate is μ_j ⁹, service rate is λ_j , and the queue capacity is Q_j . Let $y_{t,j}$ be the number of customers in queue j and let z_t be the class of the customer that is currently being served (if $z_t = 0$, this represents when there is no customer and hence, no decision to be made). Assume $\lambda_0 = 0$. The holding cost of queue j , applied to each customer in the queue, is represented by an exogenous Markov process $\{x_{t,j}\}_t$. The dynamics of the system obey the following:

1. With probability μ_j , a class $z_t = j$ customer arrives and $y_{t+1,z_t} = \min(y_{t,z_t} + 1, Q_{z_t})$.
2. With probability λ_{z_t} , the server completes serving the current customer and the queue length transitions according to $y_{t+1,z_t} = y_{t,z_t} - 1$.
3. With probability $1 - \lambda_{z_t} - \sum_j \mu_{t,j}$, no event happens and $y_{t+1,j} = y_{t,j}$ for all j .

Each time the server completes serving the current customer, an action $a_t \in \{0, 1, 2\}$ is taken to decide the class of customer to be served next, with $a_t = 0$ representing the case where no customer needs to be served. The reward function is simply the negative of the total cost: $r(x_{t,1}, x_{t,2}, y_{t,1}, y_{t,2}, a_t) = -\sum_{j=1}^2 x_{t,j} y_{t,j}$. For the frozen-state approximation, we let the slow state be $(x_{t,1}, x_{t,2})$ and the fast state be $(y_{t,1}, y_{t,2}, z_t)$.

For the nominal state approximation, we take the following approach. We solve the lower-level problem by letting $\bar{J}_t(x_1, x_2, y_1, y_2, z) = \bar{J}_{t,1}(x_1, y_1, z) + \bar{J}_{t,2}(x_2, y_2, z)$, where $\bar{J}_{t,j}(x_j, y_j, z)$ represents the reward of the optimal frozen-state policy associated with queue j . The value of $\bar{J}_{t,j}(x_j, y_j, z)$ is computed by setting $\bar{J}_{T,j}(x_j, y_j, z) = -x_j y_j$ and for other $t < T$, $\bar{J}_{t,j}(x_j, y_j, z) =$

⁹We abuse notation here by reusing μ , which was previously used in the paper to denote the upper-level policy.

$r_j(x_j, y_j, a^*) + \gamma \mathbb{E}[\bar{J}_{t+1,j}(x_j, y'_j, z')]$, where $r_j(x_j, y_j, a) = -x_j y_j$, $(y'_1, y'_2, z') = f_Y(s, a, w)$, and

$$a^* = \arg \max_{a \in \mathcal{A}} r(x_1, x_2, y_1, y_2, a) + \gamma \mathbb{E}[\bar{J}_{t+1}(x_1, x_2, y'_1, y'_2, z')].$$

We then use a multiplicative decomposition $r_j(x_j, y_j, a) = g_j(x_j)h_j(y_j)$ with $g_j(x_j) = -x_j$ and $h_j(y_j) = y_j$, and apply a multiplicative correction $g_j(x_j)/g_j(x_j^*)$ to get $\bar{J}_{t,j}(x_j, y_j, z)$ from $\bar{J}_{t,j}(x_j^*, y_j, z)$.

To make the results more easily interpretable as a function of the holding cost, we consider a case where the two classes have the same arrival rates, service rates, and capacities: $\mu_1 = \mu_2 = 0.2$, $\lambda_1 = \lambda_2 = 0.3$, and $Q_1 = Q_2 = 3$. For the cost process, let $\{a_i\}_{i=1}^6$ be six equally spaced values from the interval $[0.01, 0.2]$. Our cost process transitions on the set $\{a_i\}_{i=1}^6$ such that if $x_{t,j} = a_i$, then $x_{t+1,j} = x_{t,j}$ with probability 0.9, $x_{t+1,j} = a_{(i-1) \vee 1}$ with probability 0.05, and $x_{t+1,j} = a_{(i+1) \wedge n}$ with probability 0.05.

9.1.1 Results and Discussion for Service Allocation

Figure 4a shows the performance of the algorithms. As a function of the computational effort, Nominal FSVI and FSVI quickly outperform the other baselines. Base VI and Q-learning converge more slowly, but eventually they find policies with decent (but not superior) performance. Not surprisingly, Slow-agnostic VI plateaus quickly. These results illustrate that for the multi-class service allocation problem, although the slow state is important enough that it should not be ignored, there are drastic computational benefits of applying the frozen-state idea.

Figure 5 provides a qualitative comparison of the various policies by visualizing the actions taken in two situations: when the cost of queue 1 is lower and when the cost of queue 2 is lower. There are a few main takeaways. First, the upper level policies, along with the first 8 periods of the lower-level policies, of FSVI and Nominal FSVI resemble the Base VI policy: that is, they tend to serve customers in currently high cost queue, as long as that queue is nonempty.

Second, we observe deficiencies in the Slow-agnostic VI and Q-learning policies. By ignoring the slow state, Slow-agnostic VI's policy serves the nonempty queue when the other queue is empty, and tends to serve the shorter queue when both queues are nonempty. Q-learning also finds a suboptimal policy within the computational budget, tending to focus on the longer queue (but not the higher cost queue) in many cases.

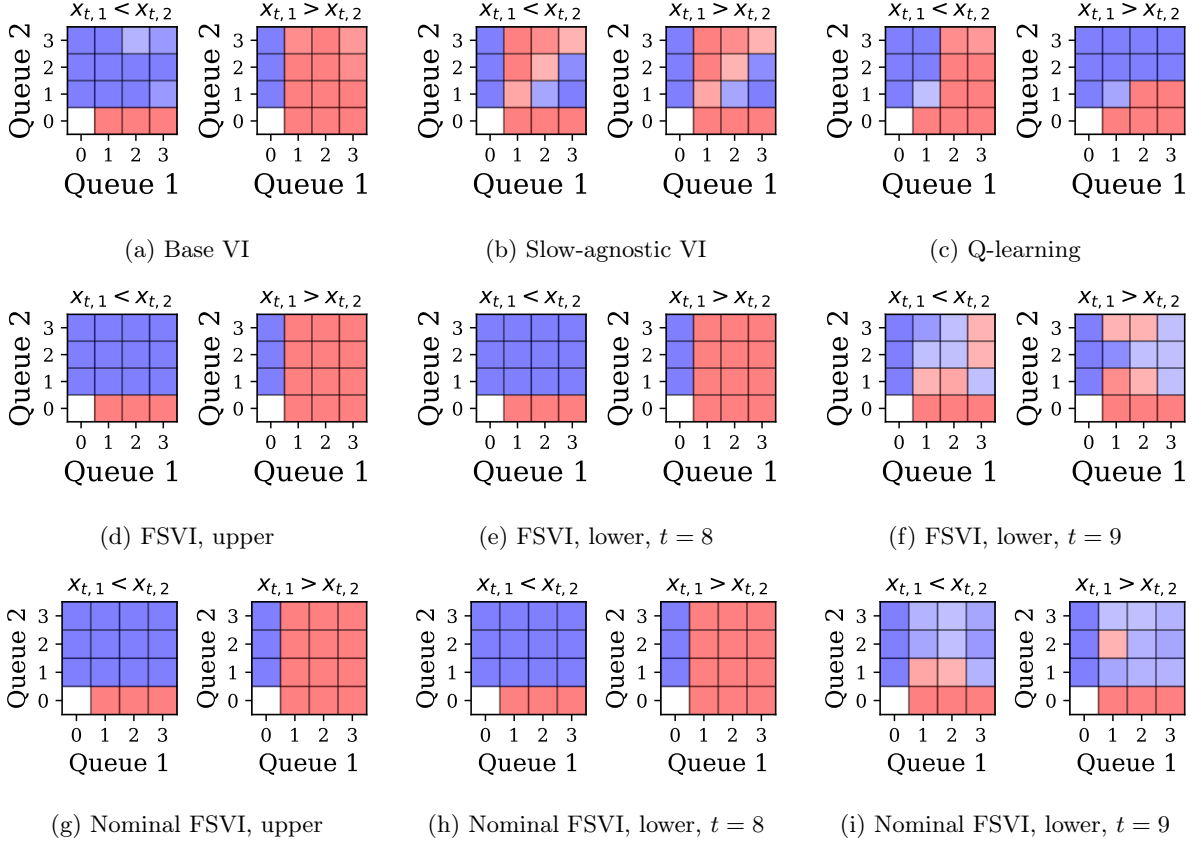


Figure 5: Visualization of the policies learned by all methods for the multi-class service allocation and queuing problem. In each plot, the x - and y -axes represent the length of the first and the second queues, respectively. A red square indicates the policy choosing to serve customers in queue 1 for the majority of runs (replications), while a blue square indicates the policy choosing to serving customers in queue 2 more often than not. The shade of the color represents the frequency of taking that action over 10 runs. For each policy, we show two situations: when the holding cost of queue 1 is lower ($x_{t,1} \leq x_{t,2}$, where we expect the optimal policy to primarily serve queue 2), and when the holding cost of queue 2 is lower ($x_{t,1} > x_{t,2}$, where we expect the optimal policy to primarily serve queue 1). Note that the first row shows methods that learn stationary policies, while the second and third rows show various snapshots of the non-stationary policies learned by FSVI and Nominal FSVI.

Third, we see that in the final lower-level period ($t = 9$), FSVI and Nominal FSVI learn poor policies due to the “end-of-horizon effect” of the zero terminal value approximation in the finite-horizon problem in the lower level. When both queues are nonempty, regardless of which queue is served, there will be no downstream impact (and the queue will not shorten). Although the frozen state approximation introduces suboptimal decisions in some periods, we can see that the good actions taken in the upper level and early stages of the lower level outweigh this issue.

9.2 Restless Multi-Armed Bandit with Environmental States

We now move on to the case of a restless multi-armed bandit (Whittle, 1988; Weber and Weiss, 1990; Killian et al., 2021; Zhang and Frazier, 2021). This problem arises in a wide variety of settings, including from machine maintenance (Smallwood and Sondik, 1973; Duan et al., 2018; Ruiz-Hernández et al., 2020), dynamic assortment planning (Brown and Smith, 2020), public health intervention decisions (Bhattacharya, 2018; Mate et al., 2020), and preventative healthcare (Lee et al., 2019; Biswas et al., 2021).

We construct a two-armed instance that features an exogenous environmental context, inspired by maintenance problems, to illustrate our frozen-state algorithms. Suppose there are two arms $j \in \{1, 2\}$ and each arm can either be operational ($y_{t,j} = 1$) or non-operational ($y_{t,j} = 0$). At the end of each period, the operator chooses whether each arm should receive an intervention (i.e., maintain or repair): $a_t = (a_{t,1}, a_{t,2})$, with each $a_{t,j} \in \{0, 1\}$. Each intervention incurs a cost of 1. The state $y_{t+1,j}$ of arm j in the next period depends on three factors: its current state $y_{t,j}$, whether it is maintained a_t , and the exogenous environment state that describes the condition of the overall system x_t . We consider 25 possible values for the environment state: $x_t \in \{0, 1, \dots, 24\}$, with x_{t+1} equal to $x_t + 2$, $x_t + 1$, x_t , $x_t - 1$ and $x_t - 2$ with probabilities 0.05, 0.15, 0.6, 0.15, and 0.05 respectively. Lower values of x_t increase the probability of of an arm becoming (and staying) non-operational; the precise values of the transition probabilities are described in Figure 6. The immediate reward function is $r(x_t, y_{t,1}, y_{t,2}, a_t) = 2 \sum_j y_{t,j} - \sum_j a_{t,i}$. We view the environment state x_t as the slow state. We use the additive nominal state approximation proposed in Section 7, which trivially applies here because the reward function does not depend on the slow state.

9.2.1 Results and Discussion for Restless Bandit

Figure 4b shows the performance of the algorithms as a function of the computational cost. The trends are similar to what we observed in Figure 4a, except here we see some notable instability of the Slow-agnostic policy. A likely explanation is given at the end of this subsection.

We use Figure 7 to visualize the final policies learned by each method. The x -axes represent the environment state, while the y -axis represents the operating state of both arms (machines). Darker gray squares on the left (right) panels indicate a high frequency of intervening arm 1 (arm 2). We

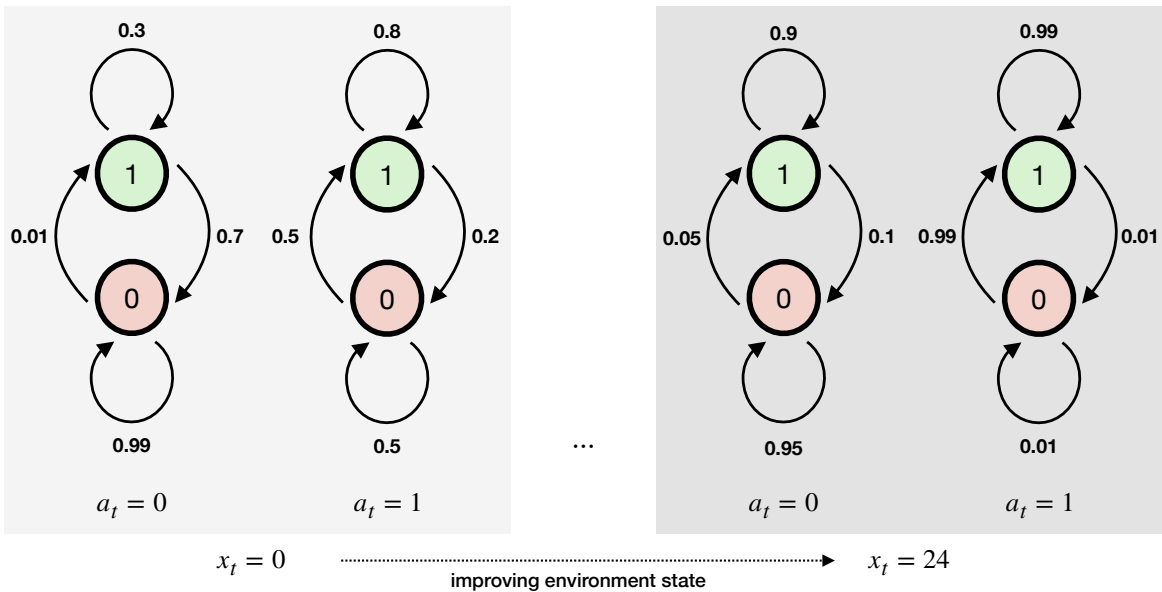


Figure 6: The transition probabilities for both arms in the two extreme environment states. When the environment is in the poorest condition $x_t = 0$, each arm stays in the non-operational state ($y_{t,j} = 0$ to $y_{t+1,j} = 0$) with probabilities 0.99 (no intervention, $a_t = 0$) and 0.5 (with intervention, $a_t = 1$). They go from operational to non-operational ($y_{t,j} = 1$ to $y_{t+1,j} = 0$) with probabilities 0.7 (no intervention, $a_t = 0$) and 0.2 (with intervention, $a_t = 1$). When the environment is in the best condition $x_t = 24$, the same probabilities are 0.95, 0.01, 0.1, and 0.01. For other values of the environment x_t , the probabilities are equally spaced between the two extreme conditions.

observe that although the Base VI policy is not particularly stable across the 10 runs, Base VI, FSVI, and Nominal FSVI all learn a policy with similar structure: intervene non-operating arms and always intervene if the environment state is smaller than 5. Given the performance plot in Figure 4b, this type of structure results in high performing policies. In addition, we observe that the frozen-state variants are significantly more stable across runs.

The Slow-agnostic policy learns to focus on non-operating arms, but its inability to distinguish between slow states hurts its performance. To understand the unstable behavior observed in Figure 4b, note that Slow-agnostic VI is only able to produce policies that apply the *same action to entire rows of the grid*. Considering what a “good” policy looks like (i.e., the Base VI, FSVI, and Nominal FSVI plots), it becomes clear that different Slow-agnostic VI policies can have dramatically different performance. For the sake of illustration, let us suppose that the FSVI policy for arm 1 is indeed optimal. Now, for Slow-agnostic VI, consider switching from the current policy that intervenes in arm 1 for (0, 0) and (0, 1) to a policy that intervenes for (0, 0), (0, 1), and (1, 0) — we suddenly go from having 5 states with suboptimal actions ($x_t \leq 4$ for $y_t = (1, 0)$) to 20 states

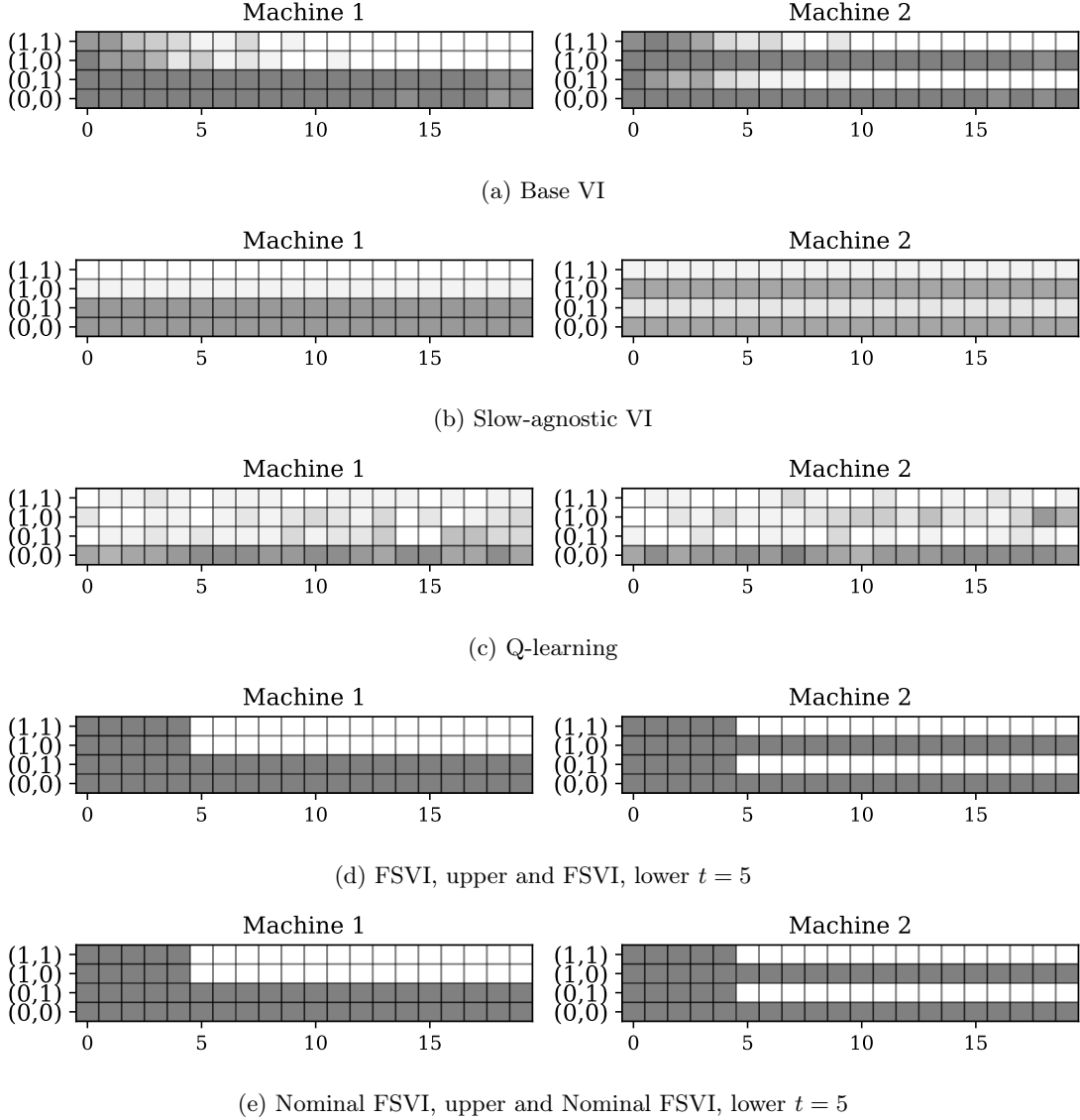


Figure 7: Visualization of the resulting policies across methods for the restless bandit. In each subplot, the x -axis is the environment state and the y -axis show the operating state of each arm (machine). The left panel shows whether to intervene machine 1, while the right panel shows whether to intervene machine 2. Darker gray squares indicate a high frequency of intervention across the 10 runs (replications) of the method. Note that in the last two subplots, the policy shown is the same policy for both the upper level and lower level, period $t = 5$.

with suboptimal actions ($x_t \geq 5$ for $y_t = (1, 0)$). In other words, the lack of flexibility of the policy space can cause widely varying performance across policies.

Finally, we note that Q-learning does not seem to have learned a policy with any notable structure, except that it more likely to intervene when both arms are in the non-operational state.

9.3 Energy Demand Response

For our last example application, we consider the problem of an energy aggregator that provides demand response to consumers, while simultaneously selling the demand reduction to the demand response market, inspired by [Khezeli et al. \(2017\)](#). At the beginning of each period t , the aggregator commits to delivering an amount of energy a_t in the *real-time* (RT) market using a forward contract, settled at the *day-ahead* (DA) price x_t . The DA price process follows a discretized Ornstein-Uhlenbeck process $x_{t+1} - x_t = c_1(c_2 - x_t) + \epsilon_{t+1}^{\text{da}}$, where $c_1 = 0.2237, c_2 = 21.4095$, estimated using data from the California Independent System Operator (CAISO).

To complete the promised delivery, the aggregator uses dynamic pricing and offers payment to elicit demand reduction, or *demand response*, from its customers. Following the model of [Khezeli et al. \(2017\)](#), if the demand reduction (which can be considered equivalent to delivering energy) falls short of the forward contract a_t , the aggregator purchases the remaining energy at the RT shortage price p_t^- , and if the demand reduction exceeds a_t , the aggregator sells the additional energy at the RT overage price p_t^+ . We model p_t^- and p_t^+ using multiplicative adjustments to the DA price x_t , i.e., $p_t^- = x_t y_t^-$ and $p_t^+ = x_t y_t^+$, with $y_t^+ < 1 < y_t^-$.

We consider a system with two (large) customers (e.g., a university or company) $m \in \{1, 2\}$. The demand response is a function of the compensation provided by the aggregator. For convenience, we represent the offered compensation as a fraction of the the DA price, i.e., $q_{t,m} = \alpha_{t,m} x_t$, where $\alpha_{t,m} \in \{0.1, 0.275, 0.45, 0.625, 0.8\}$ for each m . The vector $\alpha_t = (\alpha_{t,1}, \alpha_{t,2}, \dots, \alpha_{t,m})$ represents the pricing decisions made by the aggregator. The demand response follows a linear model $d_m(x_t, \alpha_{t,m}) = b_{m,1} + b_{m,2}(\alpha_{t,m} x_t) + \epsilon_{t+1,m}^{\text{dr}}$, where $\epsilon_{t+1,m}^{\text{dr}}$ is the noise and $b_{m,1}, b_{m,2}$ are known coefficients. The state of the system is $s_t = (x_t, y_t^-, y_t^+)$. The reward function is

$$r(x_t, y_t^+, y_t^-, a_t, \alpha_t) = x_t a_t - \sum_{m=1}^2 q_{t,m} \mathbb{E}[d_m(x_t, \alpha_{t,m})] + \mathbb{E} \left[x_t y_t^+ \left(\sum_{m=1}^2 d_m(x_t, \alpha_{t,m}) - a_t \right)^+ - x_t y_t^- \left(a_t - \sum_{m=1}^2 d_m(x_t, \alpha_{t,m}) \right)^+ \right].$$

The DA price process x_t is rounded/clipped to values in 0.1 increments between 10 and 30, and its noise term $\epsilon_{t+1}^{\text{da}}$ follows discretized normal distribution with standard deviation 1. The RT adjustment factors y_t^- and y_t^+ are each uniformly distributed over 10 equally spaced discrete values

in the ranges $[0.5, 0.8]$ and $[1.05, 1.25]$, respectively. The possible values of the pricing decisions $a_{t,m}$ are limited to the set $\{10, 12, \dots, 20\}$ in our experiment. Finally, for the demand response model, we set $b_{1,1} = 1.72, b_{1,2} = 0.55, b_{2,1} = 5.87, b_{2,2} = 0.26$, with $\epsilon_{t+1,m}^{\text{dr}}$ follows discretized normal distribution with standard deviation 0.5. With this particular set of coefficients, the impact of an additional unit of compensation offered is larger for customer 1 than for customer 2, but maximum expected demand response of customer 2 is larger than that of customer 1. For the nominal state approximation, we use a multiplicative decomposition, where the reward function is approximated as $g(x_t^*) h(x_t^*, y_t^+, y_t^-, a_t, \alpha_t)$ with $g(x_t^*) = x_t^*$ and

$$h(x_t^*, y_t^+, y_t^-, a_t, \alpha_t) = a_t - \sum_{m=1}^2 \alpha_{t,m} \mathbb{E}[d_m(x_t^*, \alpha_{t,m})] \\ + \mathbb{E} \left[y_t^+ \left(\sum_m d_m(x_t^*, \alpha_{t,m}) - a_t \right)^+ - y_t^- \left(a_t - \sum_{m=1}^2 d_m(x_t^*, \alpha_{t,m}) \right)^+ \right].$$

Instead of the additive correction term used in (22), we apply a multiplicative correction $g(x)/g(x^*)$.

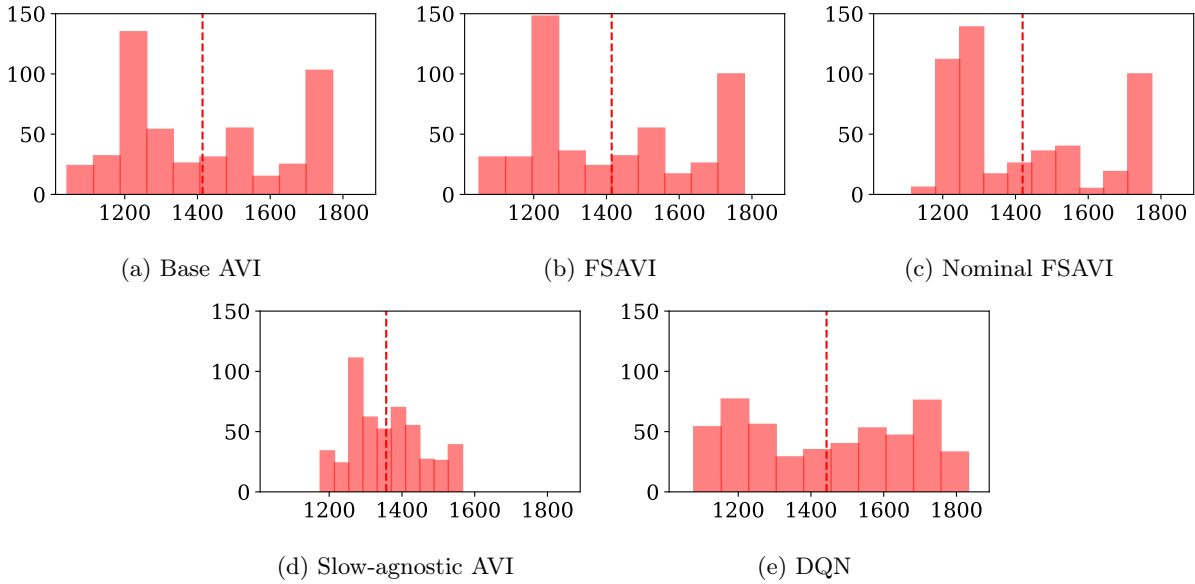


Figure 8: Histograms of the cumulative amount bid by the aggregator over 100 periods (x -axis) for each method. The y -axis are counts over 1000 simulations of the resulting policy, and the dotted vertical line shows the mean.

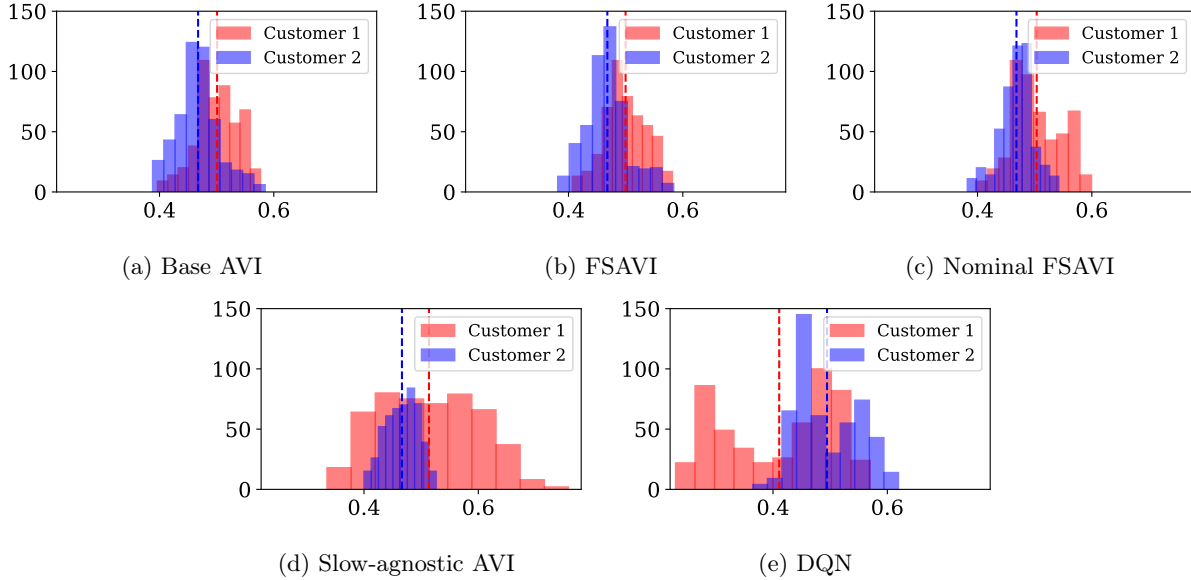


Figure 9: Histograms showing the proportion of the total amount bid that is satisfied by each customer (x -axis) over 1000 simulations of 100 periods each. The y -axis are counts over 1000 simulations, and the dotted vertical lines show the means for the customers. This is essentially an illustration of the aggregator’s pricing behavior.

9.3.1 Results and Discussion for Demand Response

The performance comparisons for the demand response problem are shown in Figure 4c. The results confirm that the trends observed for the VI-based methods in Figures 4a and 4b hold up in the AVI setting. The new methods, FSAVI and Nominal FSAVI continue to outperform the others. Base AVI and DQN both improve slowly, but continually. Slow-agnostic AVI, however, plateaus and displays a small yet still noticeable oscillation.

For a qualitative understanding of the differences between the policies, we show in Figure 8 histograms of the aggregator’s cumulative bids. Base AVI, FSAVI and Nominal FSAVI show similar bimodal bidding behavior and mean values, while the bidding behaviors of Slow-agnostic AVI and DQN deviate noticeably. The former has a much narrower distribution, while the latter shows more uniform behavior. Figure 9 shows histograms of the proportions of the overall amount bid that is satisfied by each customer. Once again, we observe Base AVI, FSAVI, and Nominal FSAVI consolidating around a particular pricing behavior, with average amount satisfied by customer 1 being slightly higher (DQN exhibits the reverse).

10 Conclusion

In this paper, we studied a new class of MDPs with a type of structure called *fast-slow* structure, motivated by practical applications where some states move slowly and are relatively less influential than others, but still important enough not to ignore them during modeling. Based on this structure, we propose a set of new algorithms based on the idea of *freezing the slow state* for several periods at a time to ease the computational burden of approximate dynamic programming. For each algorithm, we analyze the regret of the resulting policy using a novel analysis of various Bellman operators. Empirically, on three example applications, we show that our new frozen-state methods converge significantly faster to good policies than standard methods, and notably, ignoring the slow state leads to unstable training and low-performing policies. Therefore, our method can be viewed as a viable compromise between solving the full MDP (often computationally intractable) and completely ignoring states during the modeling process (computationally easy but potentially highly suboptimal in the true model).

References

- M. H. Albadi and E. F. El-Saadany. A summary of demand response in electricity markets. *Electric Power Systems Research*, 78(11):1989–1996, 2008.
- P. Ansell, K. D. Glazebrook, J. Nino-Mora, and M. O’Keeffe. Whittle’s index policy for a multi-class queueing system with convex holding costs. *Mathematical Methods of Operations Research*, 57(1):21–39, 2003.
- A. G. Barto and S. Mahadevan. Recent advances in hierarchical reinforcement learning. *Discrete Event Dynamic Systems*, 13(1-2):41–77, 2003.
- D. Bertsekas. *Dynamic programming and optimal control: Volume I*. Athena Scientific, 2012.
- D. P. Bertsekas and S. Shreve. *Stochastic optimal control: the discrete-time case*. 2004.
- D. P. Bertsekas and J. N. Tsitsiklis. *Neuro-Dynamic Programming*. Athena Scientific, 1996.
- S. Bhatnagar and J. R. Panigrahi. Actor-critic algorithms for hierarchical Markov decision processes. *Automatica*, 42(4):637–644, 2006.
- B. Bhattacharya. Restless bandits visiting villages: A preliminary study on distributing public health services. In *Proceedings of the 1st ACM SIGCAS Conference on Computing and Sustainable Societies*, pages 1–8, 2018.
- A. Biswas, G. Aggarwal, P. Varakantham, and M. Tambe. Learn to intervene: An adaptive learning policy for restless bandits in application to preventive healthcare. *arXiv preprint arXiv:2105.07965*, 2021.
- C. Boutilier, R. Dearden, and M. Goldszmidt. Stochastic dynamic programming with factored representations. *Artificial Intelligence*, 121(1-2):49–107, 2000.
- D. B. Brown and M. B. Haugh. Information relaxation bounds for infinite horizon Markov decision processes. *Operations Research*, 65(5):1355–1379, 2017.
- D. B. Brown and J. E. Smith. Index policies and performance bounds for dynamic selection problems. *Management Science*, 66(7):3029–3050, 2020.
- H. S. Chang, P. J. Fard, S. I. Marcus, and M. Shayman. Multitime scale markov decision processes. *IEEE Transactions on Automatic Control*, 48(6):976–987, 2003.
- K. Ciosek and D. Silver. Value iteration with options and state aggregation. *Planning and Learning (PAL-15)*, page 1, 2015.

- D. Cox, W. Smith, and L. Queues. Methuen and co, 1961.
- T. G. Dietterich. Hierarchical reinforcement learning with the MAXQ value function decomposition. *Journal of Artificial Intelligence Research*, 13:227–303, 2000.
- B. L. Digney. Learning hierarchical control structures for multiple tasks and changing environments. In *Proceedings of the 5th International Conference on Simulation of Adaptive Behavior on From Animals to Animats 5*, pages 321–330, 1998.
- O. D. Domingues, P. Ménard, M. Pirotta, E. Kaufmann, and M. Valko. Kernel-based reinforcement learning: A finite-time analysis. In *International Conference on Machine Learning*, pages 2783–2792. PMLR, 2021.
- C. Duan, C. Deng, A. Gharaei, J. Wu, and B. Wang. Selective maintenance scheduling under stochastic maintenance quality with multiple maintenance actions. *International Journal of Production Research*, 56(23):7160–7178, 2018.
- C. Eid, E. Koliou, M. Valles, J. Reneses, and R. Hakvoort. Time-based pricing and electricity demand response: Existing barriers and next steps. *Utilities Policy*, 40:15–25, 2016.
- J. C. Gittins. Bandit processes and dynamic allocation indices. *Journal of the Royal Statistical Society: Series B (Methodological)*, 41(2):148–164, 1979.
- J. M. Harrison. Dynamic scheduling of a multiclass queue: Discount optimality. *Operations Research*, 23(2):270–282, 1975.
- M. Jacobson, N. Shimkin, and A. Shwartz. Piecewise stationary Markov decision processes, I: Constant gain. 1999.
- A. Jonsson and A. G. Barto. A causal approach to hierarchical decomposition of factored MDPs. In *Proceedings of the 22nd International Conference on Machine Learning*, pages 401–408, 2005.
- K. Khezeli and E. Bitar. An online learning approach to buying and selling demand response. *arXiv preprint arXiv:1707.07342*, 2017.
- K. Khezeli, W. Lin, and E. Bitar. Learning to buy (and sell) demand response. *IFAC-PapersOnLine*, 50(1):6761–6767, 2017.
- J. A. Killian, A. Biswas, S. Shah, and M. Tambe. Q-learning Lagrange policies for multi-action restless bandits. In *Proceedings of the 27th ACM SIGKDD Conference on Knowledge Discovery & Data Mining*, pages 871–881, 2021.

- D. Lee and M. Vojnovic. Scheduling jobs with stochastic holding costs. *Advances in Neural Information Processing Systems*, 34, 2021.
- E. Lee, M. S. Lavieri, and M. Volk. Optimal screening for hepatocellular carcinoma: A restless bandit model. *Manufacturing & Service Operations Management*, 21(1):198–212, 2019.
- M. L. Littman, T. L. Dean, and L. P. Kaelbling. On the complexity of solving markov decision problems. In *Proceedings of the 11th Conference on Uncertainty in Artificial Intelligence*, pages 394–402, 1995.
- S. Mannor, I. Menache, A. Hoze, and U. Klein. Dynamic abstraction in reinforcement learning via clustering. In *Proceedings of the 21st International Conference on Machine Learning*, page 71, 2004.
- H. Mao, M. Schwarzkopf, S. B. Venkatakrisnan, Z. Meng, and M. Alizadeh. Learning scheduling algorithms for data processing clusters. In *Proceedings of the ACM Special Interest Group on Data Communication*, pages 270–288. 2019.
- A. Mate, J. Killian, H. Xu, A. Perrault, and M. Tambe. Collapsing bandits and their application to public health intervention. *Advances in Neural Information Processing Systems*, 33:15639–15650, 2020.
- A. McGovern and A. G. Barto. Automatic discovery of subgoals in reinforcement learning using diverse density. In *Proceedings of the 8th International Conference on Machine Learning*, pages 361–368, 2001.
- I. Menache, S. Mannor, and N. Shimkin. Q-cut-dynamic discovery of sub-goals in reinforcement learning. In *Proceedings of the 13th European Conference on Machine Learning*, pages 295–306, 2002.
- V. Mnih, K. Kavukcuoglu, D. Silver, A. Graves, I. Antonoglou, D. Wierstra, and M. Riedmiller. Playing atari with deep reinforcement learning. *arXiv preprint arXiv:1312.5602*, 2013.
- V. Mnih, K. Kavukcuoglu, D. Silver, A. A. Rusu, J. Veness, M. G. Bellemare, A. Graves, M. Riedmiller, A. K. Fidjeland, G. Ostrovski, et al. Human-level control through deep reinforcement learning. *Nature*, 518(7540):529–533, 2015.
- R. Munos and C. Szepesvári. Finite-time bounds for fitted value iteration. *Journal of Machine Learning Research*, 9(May):815–857, 2008.
- J. Ok, A. Proutiere, and D. Tranos. Exploration in structured reinforcement learning. *Advances in Neural Information Processing Systems*, 31, 2018.
- I. Osband and B. Van Roy. Near-optimal reinforcement learning in factored mdps. *Advances in Neural Information Processing Systems*, 27, 2014.

- J. R. Panigrahi and S. Bhatnagar. Hierarchical decision making in semiconductor fabs using multi-time scale Markov decision processes. In *2004 43rd IEEE Conference on Decision and Control*, volume 4, pages 4387–4392. IEEE, 2004.
- R. E. Parr and S. Russell. *Hierarchical control and learning for Markov decision processes*. University of California, Berkeley Berkeley, CA, 1998.
- W. B. Powell. *Approximate Dynamic Programming: Solving the curses of dimensionality*, volume 703. John Wiley & Sons, 2007.
- D. Precup. Temporal abstraction in reinforcement learning. *Ph.D. thesis, University of Massachusetts*, 2000.
- M. L. Puterman. *Markov decision processes: Discrete stochastic dynamic programming*. John Wiley & Sons, 2014.
- S. Ren, Y. He, and F. Xu. Provably-efficient job scheduling for energy and fairness in geographically distributed data centers. In *2012 IEEE 32nd International Conference on Distributed Computing Systems*, pages 22–31. IEEE, 2012.
- D. Ruiz-Hernández, J. M. Pinar-Pérez, and D. Delgado-Gómez. Multi-machine preventive maintenance scheduling with imperfect interventions: A restless bandit approach. *Computers & Operations Research*, 119:104927, 2020.
- Ö. Şimşek and A. G. Barto. Using relative novelty to identify useful temporal abstractions in reinforcement learning. In *Proceedings of the 21st International Conference on Machine Learning*, page 95, 2004.
- Ö. Şimşek, A. P. Wolfe, and A. G. Barto. Identifying useful subgoals in reinforcement learning by local graph partitioning. In *Proceedings of the 22nd International Conference on Machine learning*, pages 816–823, 2005.
- S. Sinclair, T. Wang, G. Jain, S. Banerjee, and C. Yu. Adaptive discretization for model-based reinforcement learning. *Advances in Neural Information Processing Systems*, 33:3858–3871, 2020.
- S. R. Sinclair, S. Banerjee, and C. L. Yu. Adaptive discretization in online reinforcement learning. *Operations Research*, 2022.
- S. P. Singh and R. C. Yee. An upper bound on the loss from approximate optimal-value functions. *Machine Learning*, 16(3):227–233, 1994.
- R. D. Smallwood and E. J. Sondik. The optimal control of partially observable Markov processes over a finite horizon. *Operations Research*, 21(5):1071–1088, 1973.

- R. Song and K. Xu. Temporal concatenation for Markov decision processes. *Probability in the Engineering and Informational Sciences*, pages 1–28, 2020.
- M. Stolle and D. Precup. Learning options in reinforcement learning. In *Proceedings of the 5th International Symposium on Abstraction, Reformulation and Approximation*, pages 212–223, 2002.
- R. S. Sutton, D. Precup, and S. Singh. Between mdps and semi-MDPs: A framework for temporal abstraction in reinforcement learning. *Artificial Intelligence*, 112(1-2):181–211, 1999.
- J. N. Tsitsiklis and B. Van Roy. Feature-based methods for large scale dynamic programming. *Machine Learning*, 22(1):59–94, 1996.
- J. A. Van Mieghem. Dynamic scheduling with convex delay costs: The generalized $c|\mu$ rule. *The Annals of Applied Probability*, pages 809–833, 1995.
- S. Wang, S. Bi, and Y.-J. A. Zhang. Demand response management for profit maximizing energy loads in real-time electricity market. *IEEE Transactions on Power Systems*, 33(6):6387–6396, 2018.
- Y. Wang, M. Poloczek, and D. R. Jiang. Subgoal-based exploration via Bayesian optimization. *arXiv preprint arXiv:1910.09143*, 2022.
- C. J. C. H. Watkins. Learning from delayed rewards. 1989.
- R. R. Weber and G. Weiss. On an index policy for restless bandits. *Journal of Applied Probability*, 27(3): 637–648, 1990.
- P. Whittle. Restless bandits: Activity allocation in a changing world. *Journal of Applied Probability*, 25(A): 287–298, 1988.
- W. Wongthatsanekorn, M. J. Realff, and J. C. Ammons. Multi-time scale Markov decision process approach to strategic network growth of reverse supply chains. *Omega*, 38(1-2):20–32, 2010.
- J. Y. Yu and S. Mannor. Arbitrarily modulated Markov decision processes. In *Proceedings of the 48th IEEE Conference on Decision and Control*, pages 2946–2953. IEEE, 2009.
- A. Zanette, A. Lazaric, M. J. Kochenderfer, and E. Brunskill. Limiting extrapolation in linear approximate value iteration. In *Advances in Neural Information Processing Systems*, pages 5616–5625, 2019.
- X. Zhang and P. I. Frazier. Restless bandits with many arms: Beating the central limit theorem. *arXiv preprint arXiv:2107.11911*, 2021.

- Z. Zhou, Z. Lan, W. Tang, and N. Desai. Reducing energy costs for ibm blue gene/p via power-aware job scheduling. In *Workshop on Job Scheduling Strategies for Parallel Processing*, pages 96–115. Springer, 2013.
- C. Zhu, J. Zhou, W. Wu, and L. Mo. Hydropower portfolios management via Markov decision process. In *IECON 2006-32nd Annual Conference on IEEE Industrial Electronics*, pages 2883–2888. IEEE, 2006.

A Proofs from Sections 3 and 4

A.1 Technical Lemmas

Lemma A.1. *Consider a (α, d_Y) -fast-slow MDP. For any states (x_0, y_0) and $(\tilde{x}_0, \tilde{y}_0)$, let (x_t, y_t) and $(\tilde{x}_t, \tilde{y}_t)$ be the states reached after t transitions under a policy $\boldsymbol{\pi} = (\pi_0, \dots, \pi_{t-1})$, i.e., $(x_t, y_t) = f^\pi(x_{t-1}, y_{t-1}, w_t)$ and $(\tilde{x}_t, \tilde{y}_t) = f^\pi(\tilde{x}_{t-1}, \tilde{y}_{t-1}, \tilde{w}_t)$. Then, for any policy $\boldsymbol{\pi}$, we have*

$$(i) \quad \|x_t - \tilde{x}_0\|_2 \leq t\alpha d_Y + \|x_0 - \tilde{x}_0\|_2,$$

$$(ii) \quad \|x_t - \tilde{x}_t\|_2 \leq 2t\alpha d_Y + \|x_0 - \tilde{x}_0\|_2,$$

$$(iii) \quad \|y_t - \tilde{y}_t\|_2 \leq 2td_Y + \|y_0 - \tilde{y}_0\|_2.$$

Proof. Lemma A.1 is a consequence of Assumption 1. □

The following two lemmas are about properties of the Bellman operators H and \tilde{H} (recall that \tilde{H} is the frozen-state version).

Lemma A.2. *For any state (x, y) and any two value functions $V, V' : \mathcal{X} \times \mathcal{Y} \rightarrow \mathbb{R}$, we have*

$$|(\tilde{H}^t V)(x, y) - (\tilde{H}^t V')(x, y)| \leq \gamma^t \max_{y \in \mathcal{Y}_x^t} |V(x, y) - V'(x, y)|,$$

where \mathcal{Y}_s^t is the set of fast states reachable from $s = (x, y)$ after t transitions of $f_Y(x, \cdot, \cdot, \cdot)$.

Proof. The result follows by the contraction property of the Bellman operators. □

Lemma A.3 (Discrepancy between H and \tilde{H}). *Consider a value function $V : \mathcal{X} \times \mathcal{Y} \rightarrow \mathbb{R}$. Suppose there exists $L_V > 0$ such that for any states (x, y) and (\tilde{x}, \tilde{y}) , it holds that $|V(x, y) - V(\tilde{x}, \tilde{y})| \leq L_V \|(x, y) - (\tilde{x}, \tilde{y})\|_2$. Then,*

$$\begin{aligned} & |(H^t V)(x, y) - (\tilde{H}^t V)(\tilde{x}, \tilde{y})| \\ & \leq \|(x, y) - (\tilde{x}, \tilde{y})\|_2 \left(L_r \sum_{i=0}^{t-1} (\gamma L_f)^i + L_V (\gamma L_f)^t \right) + \alpha d_Y \left(L_r \sum_{i=1}^{t-1} \gamma^i \sum_{j=0}^{i-1} L_f^j + L_V \gamma^t \sum_{j=0}^{t-1} L_f^j \right). \end{aligned}$$

Proof. We need to show that for each $t \geq 1$,

$$|(H^t V)(x, y) - (\tilde{H}^t V)(\tilde{x}, \tilde{y})| \leq \phi_{t,1} \|(x, y) - (\tilde{x}, \tilde{y})\|_2 + \phi_{t,2}(\alpha d y), \quad (26)$$

for coefficients $\phi_{t,1}$ and $\phi_{t,2}$ defined as

$$\phi_{t,1} = \left(L_r \sum_{i=0}^{t-1} (\gamma L_f)^i + L_V (\gamma L_f)^t \right) \quad \text{and} \quad \phi_{t,2} = \left(L_r \sum_{i=1}^{t-1} \gamma^i \sum_{j=0}^{i-1} L_f^j + L_V \gamma^t \sum_{j=0}^{t-1} L_f^j \right).$$

Let $(x', y') = (f_{\mathcal{X}}(x, y, a, w), f_{\mathcal{Y}}(x, y, a, w))$ and $(\tilde{x}', \tilde{y}') = (f_{\mathcal{X}}(\tilde{x}, \tilde{y}, a, w), f_{\mathcal{Y}}(\tilde{x}, \tilde{y}, a, w))$ be one-step transitions starting from (x, y) and (\tilde{x}, \tilde{y}) , according to the true system dynamics. For $t = 1$:

$$\begin{aligned} & |(HV)(x, y) - (\tilde{H}V)(\tilde{x}, \tilde{y})| \\ &= \left| \max_a \left\{ r(x, y, a) + \gamma \mathbb{E}[V(x', y')] \right\} - \max_{\tilde{a}} \left\{ r(\tilde{x}, \tilde{y}, \tilde{a}) + \gamma \mathbb{E}[V(\tilde{x}, \tilde{y}')] \right\} \right| \\ &\leq L_r \|(x, y) - (\tilde{x}, \tilde{y})\|_2 + \gamma \max_a \mathbb{E} |V(x', y') - V(\tilde{x}, \tilde{y}')| \\ &\leq L_r \|(x, y) - (\tilde{x}, \tilde{y})\|_2 + L_V \gamma \max_a \mathbb{E} \|(x', y') - (\tilde{x}, \tilde{y}')\|_2 \\ &= L_r \|(x, y) - (\tilde{x}, \tilde{y})\|_2 + L_V \gamma \max_a \mathbb{E} [\|(x', y') - (\tilde{x}', \tilde{y}')\|_2 + \|(\tilde{x}', \tilde{y}') - (\tilde{x}, \tilde{y}')\|_2] \\ &\leq L_r \|(x, y) - (\tilde{x}, \tilde{y})\|_2 + L_V \gamma [L_f \|(x, y) - (\tilde{x}, \tilde{y})\|_2 + \alpha d y] \\ &= \phi_{1,1} \|(x, y) - (\tilde{x}, \tilde{y})\|_2 + \phi_{1,2}(\alpha d y), \end{aligned}$$

which verifies the base case. Let us now assume that (26) holds for $t - 1$.

$$\begin{aligned} & |(H^t V)(x, y) - (\tilde{H}^t V)(\tilde{x}, \tilde{y})| \\ &= \left| \max_a \left\{ r(x, y, a) + \gamma \mathbb{E}[(HV)^{t-1}(x', y')] \right\} - \max_{\tilde{a}} \left\{ r(\tilde{x}, \tilde{y}, \tilde{a}) + \gamma \mathbb{E}[(\tilde{H}V)^{t-1}(\tilde{x}, \tilde{y}')] \right\} \right| \\ &\leq L_r \|(x, y) - (\tilde{x}, \tilde{y})\|_2 + \gamma \max_a \mathbb{E} |(HV)^{t-1}(x', y') - (\tilde{H}V)^{t-1}(\tilde{x}, \tilde{y}')| \\ &\leq L_r \|(x, y) - (\tilde{x}, \tilde{y})\|_2 + \gamma \left[\phi_{t-1,1} \|(x', y') - (\tilde{x}, \tilde{y}')\|_2 + \phi_{t-1,2}(\alpha d y) \right] \\ &\leq L_r \|(x, y) - (\tilde{x}, \tilde{y})\|_2 + \gamma \left[\phi_{t-1,1} (L_f \|(x, y) - (\tilde{x}, \tilde{y})\|_2 + \alpha d y) + \phi_{t-1,2}(\alpha d y) \right] \\ &\leq (L_r + \gamma L_f \phi_{t-1,1}) \|(x, y) - (\tilde{x}, \tilde{y})\|_2 + (\gamma \phi_{t-1,1} + \gamma \phi_{t-1,2})(\alpha d y), \end{aligned}$$

where the second inequality follows by the induction hypothesis and the third inequality follows by

the same steps as in the case of $t = 1$. It is straightforward to verify that

$$\phi_{t,1} = L_r + \gamma L_f \phi_{t-1,1} \quad \text{and} \quad \phi_{t,2} = \gamma \phi_{t-1,1} + \gamma \phi_{t-1,2},$$

which completes the induction step and the proof. \square

A.2 Proof of Proposition 3.1

We consider an MDP $\langle \mathcal{S}, \mathcal{A}, \mathcal{W}, f, r, \gamma \rangle$ and note that U^* is the unique optimal solution of the base model (5), and there exists a stationary optimal policy $\nu^*(x, y) = \arg \max U^*(x, y)$ that attains this optimal value (Bertsekas and Shreve, 2004, Proposition 4.3). Fix a state $s_0 \in \mathcal{S}$ and for $t > 0$ and a sequence of policies π_0, \dots, π_{t-1} , define the notation:

$$s_1(\pi_0) = f^{\pi_0}(s_0, w_1) \quad \text{and} \quad s_{t'+1}(\pi_0, \dots, \pi_{t'}) = f^{\pi_{t'}}(s_{t'}(\pi_0, \dots, \pi_{t'-1}), w_{t'+1})$$

for $t' \geq 1$. Therefore, we have

$$U^*(s_0) = \max_{\pi_0} r(s_0, \pi_0) + \gamma \mathbb{E}[U^*(s_1(\pi_0))] = r(s_0, \nu^*) + \gamma \mathbb{E}[U^*(s_1(\nu^*))]. \quad (27)$$

By expanding the $U^*(s_1(\pi_0))$ and $U^*(s_1(\nu^*))$ terms in (27), we have the following:

$$\begin{aligned} U^*(s_0) &= \max_{\pi_0, \pi_1} \mathbb{E} \left[r(s_0, \pi_0) + \gamma r(s_1(\pi_0), \pi_1) + \gamma^2 U^*(s_2(\pi_0, \pi_1)) \right] \\ &= \mathbb{E} \left[r(s_0, \nu) + \gamma r(s_1(\nu^*), \nu^*) + \gamma^2 U^*(s_2(\nu^*, \nu^*)) \right]. \end{aligned}$$

Let $\boldsymbol{\pi} = (\pi_0, \pi_1, \dots, \pi_{T-1})$. Repeating the expansion, we obtain:

$$U^*(s_0) = \max_{\boldsymbol{\pi}} \mathbb{E} \left[\sum_{t=0}^{T-1} \gamma^t r(s_t(\pi_0, \dots, \pi_{t-1}), \pi_t) + \gamma^T U^*(s_T(\pi_0, \dots, \pi_{T-1})) \right] \quad (28)$$

$$= \mathbb{E} \left[\sum_{t=0}^{T-1} \gamma^t r(s_t(\nu^*, \dots, \nu^*), \nu^*) + \gamma^T U^*(s_T(\nu^*, \dots, \nu^*)) \right]. \quad (29)$$

Observe that (28) is in same form as the Bellman equation (8) for the hierarchical reformulation (with T -horizon reward function R and value function \bar{U}), which has a unique optimal solution \bar{U}^* . Therefore $U^*(s_0) = \bar{U}^*(s_0)$ and (i) is proved when we recall that s_0 was chosen arbitrarily. Part (ii)

follows because by (29), it is clear that (ν^*, \dots, ν^*) solves (28) and hence also (8).

A.3 Proof of Proposition 4.1

Using (17) and (18), the difference between the two reward functions can be expanded as follows:

$$\begin{aligned}
& |\mathbb{E}[R(s_0, a, \pi^*)] - \mathbb{E}[\tilde{R}(s_0, a, J_1^*)]| \\
&= |r(x_0, y_0, a) + \gamma \mathbb{E}[(H^{T-1}U^*)(x_1, y_1)] - \gamma^T \mathbb{E}[U^*(x_T, y_T)] - r(x_0, y_0, a) - \gamma \mathbb{E}[(\tilde{H}^{T-1}\mathbf{0})(x_1, y_1)]| \\
&= \gamma |\mathbb{E}[(H^{T-1}U^*)(x_1, y_1)] - \mathbb{E}[(\tilde{H}^{T-1}\mathbf{0})(x_1, y_1)] - \gamma^{T-1} \mathbb{E}[U^*(x_T, y_T)]| \\
&\leq \underbrace{\gamma \mathbb{E}|(H^{T-1}U^*)(x_1, y_1) - (\tilde{H}^{T-1}U^*)(x_1, y_1)|}_{\text{Term A}} \\
&\quad + \underbrace{\gamma \mathbb{E}|(\tilde{H}^{T-1}U^*)(x_1, y_1) - (\tilde{H}^{T-1}\mathbf{0})(x_1, y_1) - \gamma^{T-1}U^*(x_T, y_T)|}_{\text{Term B}},
\end{aligned}$$

where (x_t, y_t) is the state obtained after transitioning from (x_0, y_0) according to the true dynamics $f = (f_x, f_y)$ for t steps. We now work on Terms A and B separately.

Noting that U^* has Lipschitz constant L_U by Assumption 2, we can apply Lemma A.3 to Term A to obtain

$$\text{Term A} \leq \alpha d_{\mathcal{Y}} \left(L_r \sum_{i=1}^{T-2} \gamma^i \sum_{j=0}^{i-1} L_f^j + \gamma^{T-1} L_U \sum_{j=0}^{T-2} L_f^j \right). \quad (30)$$

Moving on to Term B, since the reward function $r \geq 0$, it follows that $U^*(s) \geq 0$ for all s . Also, the monotonicity of \tilde{H} implies that $(\tilde{H}^{T-1}U^*) \geq (\tilde{H}^{T-1}\mathbf{0})$. Therefore, applying Lemma A.2,

$$\begin{aligned}
(\tilde{H}^{T-1}U^*)(x_1, y_1) - (\tilde{H}^{T-1}\mathbf{0})(x_1, y_1) &= |(\tilde{H}^{T-1}U^*)(x_1, y_1) - (\tilde{H}^{T-1}\mathbf{0})(x_1, y_1)| \\
&\leq \gamma^{T-1} \max_{y \in \mathcal{Y}_{s_1}^{T-1}} |U^*(x_1, y) - 0| \\
&= \gamma^{T-1} \max_{y \in \mathcal{Y}_{s_1}^{T-1}} U^*(x_1, y),
\end{aligned}$$

where $\mathcal{Y}_{s_1}^{T-1}$ is the set of fast states reachable from $s_1 = (x_1, y_1)$ after $T-1$ transitions of $f_{\mathcal{Y}}(x_1, \cdot, \cdot, \cdot)$. Let $\tilde{y}_{s_1} = \arg \max_{y \in \mathcal{Y}_{s_1}^{T-1}} U^*(x_1, y)$ be the fast state that attains the maximum. Note that \tilde{y}_{s_1} depends on s_1 , which is random. Combining with the rest of Term B, we have

$$\text{Term B} \leq \gamma \mathbb{E} |\gamma^{T-1}U^*(x_1, \tilde{y}_{s_1}) - \gamma^{T-1}U^*(x_T, y_T)|$$

$$\begin{aligned}
&\leq \max_{\omega \in \Omega} \gamma^T |U^*(x_1(\omega), \tilde{y}_{s_1}(\omega)) - U^*(x_T(\omega), y_T(\omega))| \\
&\leq \max_{\omega \in \Omega} \gamma^T L_U \left(\|x_1(\omega) - x_T(\omega)\|_2 + \|\tilde{y}_{s_1}(\omega) - y_T(\omega)\|_2 \right) \tag{31}
\end{aligned}$$

$$\leq \gamma^T L_U d_Y (\alpha + 2)(T - 1), \tag{32}$$

where (31) follows by Assumption 2 and (32) comes from Lemma A.1 (we use that $x_T(\omega)$ is $T - 1$ transitions from $x_1(\omega)$ and both $\tilde{y}_{s_1}(\omega)$ and $y_T(\omega)$ are both $T - 1$ transitions from $y_1(\omega)$). Finally, we have

$$\begin{aligned}
\text{Terms A + B} &\leq \alpha d_Y \left(L_r \sum_{i=1}^{T-2} \gamma^i \sum_{j=0}^{i-1} L_f^j + \gamma^{T-1} L_U \sum_{j=0}^{T-2} L_f^j \right) + \gamma^T L_U d_Y (\alpha + 2)(T - 1) \\
&= \alpha d_Y \left(L_r \sum_{i=1}^{T-2} \gamma^i \sum_{j=0}^{i-1} L_f^j \right) + \gamma^{T-1} L_U \left[\alpha d_Y \sum_{j=0}^{T-2} L_f^j + \gamma d_Y (\alpha + 2)(T - 1) \right]
\end{aligned}$$

which completes the proof.

B Proofs for Section 5

B.1 Technical Lemmas

Lemma B.1. *Consider two MDPs, \mathcal{M}_1 and \mathcal{M}_2 , who differ in their transition and reward functions: $\mathcal{M}_i = \langle \mathcal{S}, \mathcal{A}, \mathcal{W}, f_i, r_i, \gamma \rangle$. Let U_i^* be the optimal value function of \mathcal{M}_i . Suppose that*

(a) $|r_1(s, a) - r_2(s, a)| \leq \epsilon_r$ for all $s \in \mathcal{S}$ and $a \in \mathcal{A}$;

(b) $\|f_1(s, a, w) - f_2(s, a, w)\|_2 \leq d$ for all $s \in \mathcal{S}$, $a \in \mathcal{A}$, and $w \in \mathcal{W}$; and

(c) there exists $L_1 > 0$ such that $|U_1^*(s) - U_1^*(s')| \leq L_1 \|s - s'\|_2$ for all $s, s' \in \mathcal{S}$.

Then, the difference in optimal values of the two MDPs can be bounded as follows:

$$|U_1^*(s) - U_2^*(s)| \leq \frac{\epsilon_r + \gamma L_1 d}{1 - \gamma}$$

for all $s \in \mathcal{S}$.

Proof. Let $\hat{s} = \arg \max_{s \in \mathcal{S}} |U_1^*(s) - U_2^*(s)|$. We will analyze $|U_1^*(\hat{s}) - U_2^*(\hat{s})|$.

$$\begin{aligned}
|U_1^*(\hat{s}) - U_2^*(\hat{s})| &= \left| \max_{a_1 \in \mathcal{A}} \left\{ r_1(\hat{s}, a_1) + \gamma \mathbb{E}[U_1^*(f_1(\hat{s}, a_1, w))] \right\} - \max_{a_2 \in \mathcal{A}} \left\{ r_2(\hat{s}, a_2) + \gamma \mathbb{E}[U_2^*(f_2(\hat{s}, a_2, w))] \right\} \right| \\
&\leq \max_{a \in \mathcal{A}} |r_1(\hat{s}, a) + \gamma \mathbb{E}[U_1^*(f_1(\hat{s}, a, w))] - r_2(\hat{s}, a) - \gamma \mathbb{E}[U_2^*(f_2(\hat{s}, a, w))]| \\
&\leq \max_{a \in \mathcal{A}} |r_1(\hat{s}, a) - r_2(\hat{s}, a)| + \gamma \max_{a \in \mathcal{A}} |\mathbb{E}[U_1^*(f_1(\hat{s}, a, w))] - \mathbb{E}[U_2^*(f_2(\hat{s}, a, w))]| \\
&\leq \epsilon_r + \gamma \max_{a \in \mathcal{A}} |\mathbb{E}[U_1^*(f_1(\hat{s}, a, w)) - U_1^*(f_2(\hat{s}, a, w))]| \\
&\quad + \gamma \max_{a \in \mathcal{A}} |\mathbb{E}[U_1^*(f_2(\hat{s}, a, w)) - U_2^*(f_2(\hat{s}, a, w))]| \\
&\leq \epsilon_r + \gamma L_1 \max_{a, w} \|f_1(\hat{s}, a, w) - f_2(\hat{s}, a, w)\|_2 + \gamma \max_{s \in \mathcal{S}} |U_1^*(s) - U_2^*(s)| \\
&\leq \epsilon_r + \gamma L_1 d + \gamma |U_1^*(\hat{s}) - U_2^*(\hat{s})|.
\end{aligned}$$

Rearranging, we have

$$|U_1^*(\hat{s}) - U_2^*(\hat{s})| \leq \frac{\epsilon_r + \gamma L_1 d}{1 - \gamma},$$

which completes the proof if we recall how \hat{s} was chosen. \square

Lemma B.2. Consider two MDPs, \mathcal{M}_1 and \mathcal{M}_2 , who differ in their transition and reward functions:

$\mathcal{M}_i = \langle \mathcal{S}, \mathcal{A}, \mathcal{W}, f_i, r_i, \gamma \rangle$. Let U_i^* be the optimal value function of \mathcal{M}_i . Suppose that

(a) $|r_1(s, a) - r_2(s, a)| \leq \epsilon_r$ for all $s \in \mathcal{S}$ and $a \in \mathcal{A}$;

(b) $\|f_1(s, a, w) - f_2(s, a, w)\|_2 \leq d$ for all $s \in \mathcal{S}$, $a \in \mathcal{A}$ and $w \in \mathcal{W}$;

(c) there exists $L_1 > 0$ such that $|U_1^*(s) - U_1^*(s')| \leq L_1 \|s - s'\|_2$ for any $s, s' \in \mathcal{S}$; and

(d) $|U_1^*(s) - U_2^*(s)| \leq \epsilon_U$ for all $s \in \mathcal{S}$.

Let $\tilde{\pi}_2$ be a policy that is an approximation of the optimal policy for \mathcal{M}_2 , in the sense that:

$$\tilde{\pi}_2(s) = \arg \max_{a \in \mathcal{A}} \left\{ \tilde{r}_2(s, a) + \gamma \mathbb{E}[\tilde{U}_2(f_2(s, a, w))] \right\}, \quad (33)$$

where $|r_2(s, a) - \tilde{r}_2(s, a)| \leq \tilde{\epsilon}_r$, $\|f_2(s, a, w) - \tilde{f}_2(s, a, w)\|_2 \leq \tilde{d}$, and $|U_2^*(s) - \tilde{U}_2(s)| \leq \tilde{\epsilon}_U$ for all

$s \in \mathcal{S}$, $a \in \mathcal{A}$, and $w \in \mathcal{W}$. Then, the value of $\tilde{\pi}_2$ when implemented in \mathcal{M}_1 has regret bounded by:

$$\|U_1^* - U_1^{\tilde{\pi}_2}\|_\infty \leq \frac{2(\epsilon_r + \tilde{\epsilon}_r) + 2\gamma(\epsilon_U + \tilde{\epsilon}_U) + 2\gamma L_1(d + \tilde{d})}{1 - \gamma}.$$

This lemma is a generalization and extension of Corollary 1 of [Singh and Yee \(1994\)](#).

Proof. Let π_1^* be an optimal policy for \mathcal{M}_1 . Using (33), it follows that

$$\tilde{r}_2(s, \pi_1^*(s)) + \gamma \mathbb{E}[\tilde{U}_2(\tilde{f}_2(s, \pi_1^*(s), w))] \leq \tilde{r}_2(s, \tilde{\pi}_2(s)) + \gamma \mathbb{E}[\tilde{U}_2(\tilde{f}_2(s, \tilde{\pi}_2(s), w))]. \quad (34)$$

Set $\epsilon_U = \epsilon_U + \tilde{\epsilon}_U$, $\epsilon_r = \epsilon_r + \tilde{\epsilon}_r$. Combining parts (a) and (d) in the statement of the lemma with the approximation errors of \tilde{U}_2 and \tilde{r}_2 , we know that $U_1^*(s) - \epsilon_U \leq \tilde{U}_2(s) \leq U_1^*(s) + \epsilon_U$ and $r_1(s, a) - \epsilon_r \leq \tilde{r}_2(s, a) \leq r_1(s, a) + \epsilon_r$ for any s and a . Using these, we can lower bound both terms on the left-hand-side of (34), upper bound both terms on the right-hand-side of (34), and then rearrange to obtain

$$r_1(s, \pi_1^*(s)) - r_1(s, \tilde{\pi}_2(s)) \leq 2\epsilon_r + 2\gamma\epsilon_U + \gamma \mathbb{E}[U_1^*(\tilde{f}_2(s, \tilde{\pi}_2(s), w)) - U_1^*(\tilde{f}_2(s, \pi_1^*(s), w))]. \quad (35)$$

Let state $\hat{s} = \arg \max_{s \in \mathcal{S}} U_1^*(s) - U_1^{\tilde{\pi}_2}(s)$ be the state that achieves the largest regret (when using $\tilde{\pi}_2$ in \mathcal{M}_1). Substituting from (35) gives

$$\begin{aligned} U_1^*(\hat{s}) - U_1^{\tilde{\pi}_2}(\hat{s}) &= r_1(\hat{s}, \pi_1^*(\hat{s})) - r_1(\hat{s}, \tilde{\pi}_2(\hat{s})) + \gamma \mathbb{E}[U_1^*(f_1(\hat{s}, \pi_1^*(\hat{s}), w)) - U_1^{\tilde{\pi}_2}(f_1(\hat{s}, \tilde{\pi}_2(\hat{s}), w))] \\ &\leq 2\epsilon_r + 2\gamma\epsilon_U + \gamma \mathbb{E}[U_1^*(\tilde{f}_2(\hat{s}, \tilde{\pi}_2(\hat{s}), w)) - U_1^*(\tilde{f}_2(\hat{s}, \pi_1^*(\hat{s}), w))] \\ &\quad + \gamma \mathbb{E}[U_1^*(f_1(\hat{s}, \pi_1^*(\hat{s}), w)) - U_1^{\tilde{\pi}_2}(f_1(\hat{s}, \tilde{\pi}_2(\hat{s}), w))] \\ &= 2\epsilon_r + 2\gamma\epsilon_U + \gamma \mathbb{E}[U_1^*(\tilde{f}_2(\hat{s}, \tilde{\pi}_2(\hat{s}), w)) - U_1^*(f_1(\hat{s}, \tilde{\pi}_2(\hat{s}), w))] \\ &\quad + \gamma \mathbb{E}[U_1^*(f_1(\hat{s}, \pi_1^*(\hat{s}), w)) - U_1^*(\tilde{f}_2(\hat{s}, \pi_1^*(\hat{s}), w))] \\ &\quad + \gamma \mathbb{E}[U_1^*(f_1(\hat{s}, \tilde{\pi}_2(\hat{s}), w)) - U_1^{\tilde{\pi}_2}(f_1(\hat{s}, \tilde{\pi}_2(\hat{s}), w))] \\ &\leq 2\epsilon_r + 2\gamma\epsilon_U + 2\gamma L_1(d + \tilde{d}) + \gamma(U_1^*(\hat{s}) - U_1^{\tilde{\pi}_2}(\hat{s})), \end{aligned}$$

where we have used property (c) and that $\|f_1(s, a, w) - \tilde{f}_2(s, a, w)\|_2 \leq d + \tilde{d}$. Therefore, we rearrange

to see that

$$U_1^*(\hat{s}) - U_1^{\tilde{\pi}_2}(\hat{s}) \leq \frac{2\epsilon_r + 2\gamma\epsilon_U + 2\gamma L_1(d + \tilde{d})}{1 - \gamma},$$

completing the proof. \square

B.2 Proof of Lemma 5.1

To analyze $\mathcal{R}(\mu, \pi) = \|\bar{U}^* - \bar{U}^\mu(\pi)\|_\infty$, we will consider two MDPs that operate on the T -period timescale, one with optimal value \bar{U}^* and the other with optimal value $V^*(J_1, \pi)$. The reason to study an MDP with optimal value $V^*(J_1, \pi)$ is because μ can be viewed as an *approximation* to the optimal policy for the second MDP, as suggested in (20). Since both MDPs are defined on the T -period timescale, the transition functions are defined using T -period noise sequences $\mathbf{w} = (w_1, w_2, \dots, w_T)$.

- For \bar{U}^* , let $\mathcal{M}_1 = \langle \mathcal{S}, \mathcal{A}, \mathcal{W}, f_1, r_1, \gamma^T \rangle$ be the MDP associated with the base model reformulation (8), but with the lower-level policy fixed to be π^* . The reward function r_1 is $r_1(s, a) = \mathbb{E}[R(s, a, \pi^*)]$. Given a T -period noise sequence \mathbf{w} , an initial state s , and action a , the “next” state $f_1(s, a, \mathbf{w}) = s_T(a, \pi^*)$ is the state obtained by first taking action a in state s and then following policy π^* for the next $T - 1$ steps.
- For $V^*(J_1, \pi)$, let $\mathcal{M}_2 = \langle \mathcal{S}, \mathcal{A}, \mathcal{W}, f_2, r_2, \gamma^T \rangle$ be the MDP associated with the frozen-state hierarchical approximation (14), where r_2 is defined as $r_2(s, a) = \mathbb{E}[\tilde{R}(s, a, J_1)]$. The transition function f_2 is defined in the same way as f_1 except we replace π^* by π .

Let $\epsilon_r(\pi^*, J_1) = \max_{s,a} |\mathbb{E}[R(s, a, \pi^*)] - \mathbb{E}[\tilde{R}(s, a, J_1)]|$, so that we have $|r_1(s, a) - r_2(s, a)| \leq \epsilon_r(\pi^*, J_1)$. Noting that the first steps of f_1 and f_2 are the same (action a in state s with w_1 revealed), applying parts (ii) and (iii) of Lemma A.1, the maximum discrepancy between f_1 and f_2 is:

$$\|f_1(s, a, \mathbf{w}) - f_2(s, a, \mathbf{w})\|_2 \leq d(\alpha, d_Y, T) := 2(\alpha + 1)d_Y(T - 1).$$

Applying Lemma B.1, we see that

$$\|\bar{U}^* - V^*(J_1, \pi)\|_\infty \leq \frac{1}{1 - \gamma^T} \left(\epsilon_r(\pi^*, J_1) + \gamma^T L_U d(\alpha, d_Y, T) \right).$$

We also need to account for the fact that μ is greedy with respect to V , an approximation of the optimal value of \mathcal{M}_2 . More precisely, μ is greedy with respect to $r_2(s, a) = \mathbb{E}[\tilde{R}(s_0, a, J_1)]$, $f_2(s, a, \mathbf{w}) = s_T(a, \boldsymbol{\pi})$, and value function V . We can thus apply Lemma B.2 with $\epsilon_r = \epsilon_r(\boldsymbol{\pi}^*, J_1)$, $d = d(\alpha, d_Y, T)$, $L_1 = L_U$, $\epsilon_U = \|\bar{U}^* - V^*(J_1, \boldsymbol{\pi})\|_\infty$, and $\tilde{\epsilon}_U = \|V - V^*(J_1, \tilde{\boldsymbol{\pi}})\|_\infty$. Collecting terms completes the proof.

C Proofs for Section 6

C.1 Technical Lemmas

Lemma C.1. *Consider an MDP $\langle \mathcal{S}, \mathcal{A}, \mathcal{W}, f, r, \gamma \rangle$ with reward function r taking values in $[0, r_{\max}]$. Suppose the optimal value function is U^* and the associated Bellman operator is F . Fix any initial value function such that $0 \leq U_0(s) \leq r_{\max}/(1 - \gamma)$ for all s and let $U^k = F^k U_0$ be the result after iteration k of value iteration. Then, it holds that*

$$\|U^k - U^*\|_\infty \leq \frac{\gamma^k r_{\max}}{1 - \gamma}.$$

Proof. This is a standard result that follows from the contraction property of F and the fact that $U^k = F U^{k-1}$. Therefore,

$$\|U^k - U^*\|_\infty = \|H U^{k-1} - H U^*\|_\infty \leq \gamma \|U^{k-1} - U^*\|_\infty \leq \gamma^k \|U^0 - U^*\|_\infty \leq \frac{\gamma^k r_{\max}}{1 - \gamma},$$

where in the last step, we used $0 \leq U^*(s) \leq r_{\max}/(1 - \gamma)$ for all s . □

Lemma C.2 (Proposition 6.1 of Bertsekas and Tsitsiklis (1996)). *Consider an MDP $\langle \mathcal{S}, \mathcal{A}, \mathcal{W}, f, r, \gamma \rangle$ with optimal value function U^* . Suppose that ν is a policy that is greedy with respect to another value function U :*

$$\nu(s) = \arg \max_a \{r(s, a) + \mathbb{E}[U(f(s, a, w))]\}.$$

If $\|U - U^\|_\infty \leq \varepsilon$, then the performance of ν is bounded as follows:*

$$\|U^\nu - U^*\|_\infty \leq \frac{2\gamma\varepsilon}{1 - \gamma}.$$

Lemma C.3. Let $V^k(J_1^*, \boldsymbol{\pi}^*)$ be the value function approximation obtained from running FSVI for k iterations. Then, the “value iteration error” is given by

$$\|V^k(J_1^*, \boldsymbol{\pi}^*) - V^*(J_1^*, \boldsymbol{\pi}^*)\|_\infty \leq \frac{\gamma^{kT} r_{\max}}{1 - \gamma}.$$

Proof. Consider the upper-level MDP. Note that the discount factor is γ^T and the T -horizon reward function

$$\tilde{R}(s_0, a, J_1^*) \in \left[0, \frac{1 - \gamma^T}{1 - \gamma} r_{\max}\right].$$

The result follows by Lemma C.1. □

C.2 Proof of Proposition 6.1

Since ν_k is greedy with respect to U_k , we can apply Lemmas C.1 and C.2 to obtain

$$\|U^{\nu_k} - U^*\|_\infty \leq \frac{2\gamma}{1 - \gamma} \frac{\gamma^k r_{\max}}{1 - \gamma} = \frac{2r_{\max}\gamma^{k+1}}{(1 - \gamma)^2}.$$

C.3 Proof of Theorem 6.1

We apply Lemma 5.1 with $\boldsymbol{\pi} = \tilde{\boldsymbol{\pi}}^*$, $J_1 = J_1^*$, and $V = V^k(J_1^*, \boldsymbol{\pi}^*)$. The result follows by combining it with the result of Lemma C.3 and noting that by Proposition 4.1, $\epsilon_r(\boldsymbol{\pi}^*, J_1^*) \leq \epsilon_r(\gamma, \alpha, d_{\mathcal{Y}}, \mathbf{L}, T)$.

D Proofs for Section 7

D.1 Proof of Lemma 7.1

First, we note that $\bar{J}_t(x, y)$ *nearly* satisfies the Bellman equation for the separable MDP, with the exception of a next state transition that is based on x^* . Let $y'(x, y, a) = f_{\mathcal{Y}}(x, y, a, w)$ and $\Delta_g(x) = g(x) - g(x^*)$. We have:

$$\begin{aligned} \bar{J}_t(x, y) &= \sum_{i=0}^{T-t-1} \gamma^i \Delta_g(x) + \max_a \left\{ g(x^*) + h(y, a) + \gamma \mathbb{E}[\bar{J}_{t+1}(x^*, y'(x^*, y, a))] \right\} \\ &= \sum_{i=0}^{T-t-1} \gamma^i \Delta_g(x) + \max_a \left\{ g(x^*) + h(y, a) + \gamma \mathbb{E} \left[\bar{J}_{t+1}(x, y'(x^*, y, a)) - \sum_{i=0}^{T-t-2} \gamma^i \Delta_g(x) \right] \right\} \end{aligned}$$

$$\begin{aligned}
&= \sum_{i=0}^{T-t-1} \gamma^i \Delta_g(x) + \max_a \left\{ g(x^*) + h(y, a) + \gamma \mathbb{E} \left[\bar{J}_{t+1}(x, y'(x^*, y, a)) - \sum_{i=0}^{T-t-2} \gamma^i \Delta_g(x) \right] \right\} \\
&= \Delta_g(x) + \max_a \left\{ g(x^*) + h(y, a) + \gamma \mathbb{E} [\bar{J}_{t+1}(x, y'(x^*, y, a))] \right\} \\
&= \max_a \left\{ g(x) + h(y, a) + \gamma \mathbb{E} [\bar{J}_{t+1}(x, y'(x^*, y, a))] \right\}. \tag{36}
\end{aligned}$$

The main proof is by backward induction. Consider states (x, y) and (\tilde{x}, \tilde{y}) . When $t = T - 1$, the difference between the two values is

$$\begin{aligned}
|\bar{J}_{T-1}(x, y) - J_{T-1}^*(\tilde{x}, \tilde{y})| &= |g(x) - g(x^*) + \max_a (g(x^*) + h(y, a)) - \max_a r(\tilde{x}, \tilde{y}, \tilde{a})| \\
&\leq \max_a |g(x) + h(y, a) - r(\tilde{x}, \tilde{y}, a)| \\
&\leq \max_a |g(x) + h(y, a) - r(x, y, a)| + \max_a |r(x, y, a) - r(\tilde{x}, \tilde{y}, a)| \\
&\leq \zeta + L_r (\|x - \tilde{x}\|_2 + \|y - \tilde{y}\|_2),
\end{aligned}$$

where the last inequality follows from Assumption 3 and (2). Suppose that the desired result holds for period t , i.e., we have

$$\begin{aligned}
|\bar{J}_t(x, y) - J_t^*(\tilde{x}, \tilde{y})| &\leq \left(\sum_{i=0}^{T-t-1} \gamma^i \right) (\zeta + L_r \|x - \tilde{x}\|_2) + \left(\sum_{i=0}^{T-t-1} \gamma^i L_f^i \right) L_r \|y - \tilde{y}\|_2 \\
&\quad + \left(\sum_{i=1}^{T-t-1} L_f^i \sum_{j=i}^{T-t-1} \gamma^j \right) L_r \|x^* - \tilde{x}\|_2. \tag{37}
\end{aligned}$$

Then for period $t - 1$, the value difference can be expanded as

$$\begin{aligned}
&|\bar{J}_{t-1}(x, y) - J_{t-1}^*(\tilde{x}, \tilde{y})| \\
&= \left| \max_a \left\{ g(x) + h(y, a) + \gamma \mathbb{E} [\bar{J}_t(x, y'(x^*, y, a))] \right\} - \max_a \left\{ r(\tilde{x}, \tilde{y}, \tilde{a}) + \gamma \mathbb{E} [J_t^*(\tilde{x}, y'(\tilde{x}, \tilde{y}, \tilde{a}))] \right\} \right| \\
&\leq \underbrace{\max_a |g(x) + h(y, a) - r(\tilde{x}, \tilde{y}, a)|}_{\text{Term A}} + \underbrace{\gamma \max_a \left| \mathbb{E} [\bar{J}_t(x, f_{\mathcal{Y}}(x^*, y, a, w)) - J_t^*(\tilde{x}, f_{\mathcal{Y}}(\tilde{x}, \tilde{y}, a, w))] \right|}_{\text{Term B}}, \tag{38}
\end{aligned}$$

where we used (36) in the equality above. It is easy to see that by Assumption 3

$$\text{Term A} \leq \zeta + L_r (\|x - \tilde{x}\|_2 + \|y - \tilde{y}\|_2).$$

Noting that

$$\|f_{\mathcal{Y}}(x^*, y, a, w) - f_{\mathcal{Y}}(\tilde{x}, \tilde{y}, a, w)\|_2 \leq L_f (\|x^* - \tilde{x}\|_2 + \|y - \tilde{y}\|_2),$$

we see from the induction hypothesis (37) that

$$\begin{aligned} \text{Term B} &\leq \gamma \left[\left(\sum_{i=0}^{T-t-1} \gamma^i \right) (\zeta + L_r \|x - \tilde{x}\|_2) + \left(\sum_{i=0}^{T-t-1} \gamma^i L_f^i \right) L_r L_f (\|x^* - \tilde{x}\|_2 + \|y - \tilde{y}\|_2) \right. \\ &\quad \left. + \left(\sum_{i=1}^{T-t-1} L_f^i \sum_{j=i}^{T-t-1} \gamma^j \right) L_r \|x^* - \tilde{x}\|_2 \right] \\ &= \left(\sum_{i=1}^{T-t} \gamma^i \right) (\zeta + L_r \|x - \tilde{x}\|_2) + \left(\sum_{i=1}^{T-t} \gamma^i L_f^i \right) L_r (\|x^* - \tilde{x}\|_2 + \|y - \tilde{y}\|_2) \\ &\quad + \left(\sum_{i=1}^{T-t-1} L_f^i \sum_{j=i+1}^{T-t} \gamma^j \right) L_r \|x^* - \tilde{x}\|_2 \\ &= \left(\sum_{i=1}^{T-t} \gamma^i \right) (\zeta + L_r \|x - \tilde{x}\|_2) + \left(\sum_{i=1}^{T-t} \gamma^i L_f^i \right) L_r \|y - \tilde{y}\|_2 + \left(\sum_{i=1}^{T-t} L_f^i \sum_{j=i}^{T-t} \gamma^j \right) L_r \|x^* - \tilde{x}\|_2, \end{aligned}$$

where the last equality is obtained by from

$$\sum_{i=1}^{T-t} L_f^i \sum_{j=i}^{T-t} \gamma^j = \sum_{i=1}^{T-t} \gamma^i L_f^i + \sum_{i=1}^{T-t-1} L_f^i \sum_{j=i+1}^{T-t} \gamma^j.$$

Combining Terms A and B completes the proof.

D.2 Proof of Proposition 7.1

The difference of the reward functions $|\mathbb{E}[\tilde{R}(s_0, a, J_1^*)] - \mathbb{E}[\tilde{R}(s_0, a, \bar{J}_1^*)]|$ can be expanded as follows,

$$\begin{aligned} |\mathbb{E}[\tilde{R}(s_0, a, J_1^*)] - \mathbb{E}[\tilde{R}(s_0, a, \bar{J}_1)]| &= \gamma |\mathbb{E}[J_1^*(f(s_0, a, w))] - \mathbb{E}[\bar{J}_1(f(s_0, a, w))]| \\ &\leq \sum_{i=1}^{T-1} \gamma^i \zeta + \left(\sum_{i=1}^{T-2} L_f^i \sum_{j=i+1}^{T-1} \gamma^j \right) L_r \max_x \|x^* - x\|_2, \end{aligned}$$

where the inequality is by Lemma 7.1.

E Proofs for Section 8

E.1 Technical Lemmas

Lemma E.1. *For any vectors $J \in \mathbb{R}^N$ and $J' \in \mathbb{R}^N$, it holds that*

$$\|(\Phi\Phi^\dagger)(J) - (\Phi\Phi^\dagger)(J')\|_\infty \leq \kappa \|J - J'\|_\infty$$

Proof. For simplicity, let $D = \Phi[\Phi^\dagger(J) - \Phi^\dagger(J')]$ be the term inside the norm on the left hand side. Then, for any state s , we have $|D(s)| = \phi^\top(s)[\Phi^\dagger(J) - \Phi^\dagger(J')]$. We select $\theta_1(s), \theta_1(s), \dots, \theta_M(s) \in \mathbb{R}$ that satisfy Assumption 4, obtaining

$$\begin{aligned} |D(s)| &= \left| \kappa \left(\sum_{m=1}^M \theta_m(s) \phi^\top(s_m) \right) (\Phi^\dagger(J) - \Phi^\dagger(J')) \right| \\ &\leq \kappa \max_m |\phi^\top(s_m) (\Phi^\dagger(J)) - \Phi^\dagger(J')| \\ &= \kappa \max_m |D(s_m)| \\ &= \kappa \max_m |J(s_m) - J'(s_m)| \\ &\leq \kappa \|J - J'\|_\infty \end{aligned}$$

where the third equality uses the fact that s_m is a pre-selected state. \square

Lemma E.2. *Given a lower-level value function $\hat{J}(\omega_{t+1})$, recall that one approximate Bellman step in the lower level of FSAVI yields $\hat{J}(\omega_t) = \Phi\Phi^\dagger\bar{H}\hat{J}(\omega_{t+1})$ in the value function space. If $\omega_T = \mathbf{0}$,*

$$\|\hat{J}(\omega_1)\|_\infty \leq \kappa r_{\max} \sum_{i=0}^{T-1} (\kappa\gamma)^i = \frac{(\kappa\gamma)^T - 1}{\kappa\gamma - 1} \kappa r_{\max}.$$

Moreover, the upper-level reward function can be bounded as follows:

$$|\mathbb{E}[\tilde{R}(s_0, a, \hat{J}_1(\omega_1))]| \leq \frac{(\kappa\gamma)^{T+1} - 1}{\kappa\gamma - 1} \kappa r_{\max}.$$

Proof. The proof follows by Assumption 4 and some manipulation:

$$\begin{aligned}
|\hat{J}(\boldsymbol{\omega}_t)(s)| &= \left| \kappa \left(\sum_{m=1}^M \theta_m(s) \boldsymbol{\phi}^\top(s_m) \right) (\Phi^\dagger \bar{H} \hat{J}(\boldsymbol{\omega}_{t+1})) \right| \\
&\leq \kappa \max_m |\boldsymbol{\phi}^\top(s_m) (\Phi^\dagger \bar{H} \hat{J}(\boldsymbol{\omega}_{t+1}))| \\
&= \kappa \max_m |(\bar{H} \hat{J}(\boldsymbol{\omega}_t))(s_m)| \\
&= \kappa r_{\max} + \kappa \gamma \|\hat{J}(\boldsymbol{\omega}_{t+1})\|_\infty.
\end{aligned}$$

Applying the above inequality $T - 1$ times yields the first result. Next, we see that

$$\begin{aligned}
|\mathbb{E}[\tilde{R}(s_0, a, \hat{J}_1(\boldsymbol{\omega}_1))]| &\leq r_{\max} + \gamma \|\hat{J}(\boldsymbol{\omega}_1)\|_\infty \\
&\leq \kappa r_{\max} + \kappa \gamma \|\hat{J}(\boldsymbol{\omega}_1)\|_\infty \\
&\leq \kappa r_{\max} \sum_{i=0}^T (\kappa \gamma)^i,
\end{aligned}$$

where we used the fact that $\kappa \geq 1$ in the second inequality. □

Lemma E.3. *Suppose $(\boldsymbol{\omega}_1^*, \boldsymbol{\omega}_2^*, \dots, \boldsymbol{\omega}_T^*)$ satisfies $\boldsymbol{\omega}_t^* = \bar{H}' \boldsymbol{\omega}_{t+1}^*$ for all t . Then, we have*

$$\|J_t^* - \hat{J}_t(\boldsymbol{\omega}_t^*)\|_\infty \leq \left(1 + \frac{\gamma + 1}{\gamma} \sum_{i=1}^{T-t} (\kappa \gamma)^i \right) \varepsilon_{\text{low}} = \left(\frac{1 + \kappa}{1 - \kappa \gamma} - \frac{(\kappa \gamma)^T (1 + \gamma)}{\gamma - \kappa \gamma^2} \right) \varepsilon_{\text{low}}$$

a bound on the error of the value function approximation.

Proof. Let $\varepsilon' = \varepsilon_{\text{low}} + \delta$ for some $\delta > 0$. For each t , choose a parameter vector $\bar{\boldsymbol{\omega}}_t \in \mathbb{R}^M$ such that $\|J_t^* - \hat{J}_t(\bar{\boldsymbol{\omega}}_t)\|_\infty < \varepsilon'$, which is possible by the definition of ε_{low} . Then, it holds that

$$\begin{aligned}
\|\hat{J}_t(\bar{\boldsymbol{\omega}}_t) - \Phi \bar{H}'(\bar{\boldsymbol{\omega}}_{t+1})\|_\infty &= \|\Phi \bar{\boldsymbol{\omega}}_t - \Phi \Phi^\dagger \bar{H} \hat{J}_{t+1}(\bar{\boldsymbol{\omega}}_{t+1})\|_\infty \\
&= \|\Phi \Phi^\dagger \Phi \bar{\boldsymbol{\omega}}_t - \Phi \Phi^\dagger \bar{H} \hat{J}_{t+1}(\bar{\boldsymbol{\omega}}_{t+1})\|_\infty \\
&\leq \kappa \|\Phi \bar{\boldsymbol{\omega}}_t - \bar{H} \hat{J}_{t+1}(\bar{\boldsymbol{\omega}}_{t+1})\|_\infty \\
&= \kappa \|\hat{J}_t(\bar{\boldsymbol{\omega}}_t) - \bar{H} \hat{J}_{t+1}(\bar{\boldsymbol{\omega}}_{t+1})\|_\infty \\
&\leq \kappa \left(\|\hat{J}_t(\bar{\boldsymbol{\omega}}_t) - J_t^*\|_\infty + \|J_t^* - \bar{H} \hat{J}_{t+1}(\bar{\boldsymbol{\omega}}_{t+1})\|_\infty \right) \\
&< \kappa \left(\varepsilon' + \|\bar{H} J_{t+1}^* - \bar{H} \hat{J}_{t+1}(\bar{\boldsymbol{\omega}}_{t+1})\|_\infty \right)
\end{aligned} \tag{39}$$

$$\begin{aligned}
&\leq \kappa \left(\varepsilon' + \gamma \|J_{t+1}^* - \hat{J}_{t+1}(\bar{\omega}_{t+1})\|_\infty \right) \\
&< \kappa(\gamma + 1) \varepsilon'.
\end{aligned} \tag{40}$$

where (39) is by Lemma E.1 and (40) follows by the contraction property of \bar{H} . The next step is to quantify the difference between $\hat{J}_t(\bar{\omega}_t)$ and $\hat{J}_t(\omega_t^*)$. Let $\varepsilon'' = \kappa(\gamma + 1) \varepsilon'$.

$$\begin{aligned}
\|\hat{J}_t(\bar{\omega}_t) - \hat{J}_t(\omega_t^*)\|_\infty &\leq \|\hat{J}_t(\bar{\omega}_t) - \Phi \bar{H}'(\bar{\omega}_{t+1})\|_\infty + \|\Phi \bar{H}'(\bar{\omega}_{t+1}) - \hat{J}_t(\omega_t^*)\|_\infty \\
&\leq \varepsilon'' + \|\Phi \Phi^\dagger \bar{H} \hat{J}_{t+1}(\bar{\omega}_{t+1}) - \Phi \Phi^\dagger \bar{H} \hat{J}_{t+1}(\omega_{t+1}^*)\|_\infty \\
&\leq \varepsilon'' + \frac{\gamma'}{\gamma} \|\bar{H} \hat{J}_{t+1}(\bar{\omega}_{t+1}) - \bar{H} \hat{J}_{t+1}(\omega_{t+1}^*)\|_\infty
\end{aligned} \tag{41}$$

$$\leq \varepsilon'' + \gamma' \|\hat{J}_{t+1}(\bar{\omega}_{t+1}) - \hat{J}_{t+1}(\omega_{t+1}^*)\|_\infty \tag{42}$$

$$\leq \varepsilon'' + \gamma' \left(\varepsilon'' + \gamma' \|\hat{J}_{t+2}(\bar{\omega}_{t+2}) - \hat{J}_{t+2}(\omega_{t+2}^*)\|_\infty \right)$$

$$\leq \dots$$

$$\begin{aligned}
&\leq \varepsilon'' \sum_{i=0}^{T-t-1} (\gamma')^i + (\gamma')^{T-t} \|\hat{J}_T(\bar{\omega}_T) - \hat{J}_T(\omega_T^*)\|_\infty \\
&= \frac{\gamma + 1}{\gamma} \varepsilon' \sum_{i=1}^{T-t} (\gamma')^i,
\end{aligned} \tag{43}$$

where (41) is by Lemma E.1, (42) is by the contraction property of \bar{H} , and (43) because $\omega_T^* = \bar{\omega}_T = \mathbf{0}$ (since $J_T(s) = 0$ for all s). Therefore,

$$\begin{aligned}
\|J_t^* - \hat{J}_t(\omega_t^*)\|_\infty &\leq \|J_t^* - \hat{J}_t(\bar{\omega}_t)\|_\infty + \|\hat{J}_t(\bar{\omega}_t) - \hat{J}_t(\omega_t^*)\|_\infty \\
&\leq \varepsilon' \left(1 + \frac{\gamma + 1}{\gamma} \sum_{i=1}^{T-t} (\gamma')^i \right) \\
&= \varepsilon' \left(1 + \frac{\gamma + 1}{\gamma} \sum_{i=1}^{T-t} (\kappa\gamma)^i \right) \\
&= \varepsilon' \left(1 + \frac{\gamma + 1}{\gamma} \frac{\kappa\gamma - (\kappa\gamma)^T}{1 - \kappa\gamma} \right) \\
&= \varepsilon' \left(\frac{1 + \kappa}{1 - \kappa\gamma} - \frac{(\kappa\gamma)^T (1 + \gamma)}{\gamma - \kappa\gamma^2} \right).
\end{aligned}$$

Since δ can be arbitrarily small, the proof is complete. \square

Lemma E.4. *Given an upper-level value function $\hat{V}(\boldsymbol{\beta}_i)$, recall that one approximate Bellman step in the upper level of FSAVI yields $\hat{V}(\boldsymbol{\beta}_{i+1}) = \Phi\Phi^\dagger F_{\boldsymbol{\omega}^*}\hat{V}(\boldsymbol{\beta}_i)$ in the value function space. We have*

$$\|\hat{V}(\boldsymbol{\beta}^*)\| \leq \frac{\kappa^2 - \kappa^2(\kappa\gamma)^{T+1}}{(1 - \kappa\gamma^T)(1 - \kappa\gamma)} r_{\max},$$

where $\boldsymbol{\beta}^*$ is a fixed point of $F'_{\boldsymbol{\omega}^*}$.

Proof. Again, the proof follows by Assumption 4 and some manipulation:

$$\begin{aligned} |\hat{V}(\boldsymbol{\beta}_{i+1})(s)| &= \left| \kappa \left(\sum_{m=1}^M \theta_m(s) \phi^\top(s_m) \right) (\Phi^\dagger F_{\boldsymbol{\omega}} \hat{V}(\boldsymbol{\beta}_i)) \right| \\ &\leq \kappa \max_m |\phi^\top(s_m) (\Phi^\dagger F_{\boldsymbol{\omega}} \hat{V}(\boldsymbol{\beta}_i))| \\ &= \kappa \max_m |(F_{\boldsymbol{\omega}} \hat{V}(\boldsymbol{\beta}_i))(s_m)| \\ &\leq \kappa R_{\max} + \kappa\gamma^T \|\hat{V}(\boldsymbol{\beta}_i)\|_\infty, \end{aligned}$$

where R_{\max} is an upper bound on $|\mathbb{E}[\tilde{R}(s_0, a, \hat{J}_1(\boldsymbol{\omega}_1))]|$ from Lemma E.2. Starting with $\boldsymbol{\beta}_i = \mathbf{0}$ and applying the inequality repeatedly, we see that

$$\|\hat{V}(\boldsymbol{\beta}^*)\|_\infty \leq \kappa R_{\max} \sum_{j=0}^{\infty} (\kappa\gamma^T)^j \leq \frac{\kappa R_{\max}}{1 - \kappa\gamma^T},$$

which completes the proof. □

Lemma E.5. *For any $\boldsymbol{\omega}$, the parameter space Bellman operator for the upper-level problem $F'_{\boldsymbol{\omega}} = \Phi^\dagger \circ F_{\boldsymbol{\omega}} \circ \Phi$ is a γ' -contraction with respect to a norm $\|\cdot\|_\Phi$ on \mathbb{R}^M defined by $\|\boldsymbol{\beta}\|_\Phi = \|\Phi\boldsymbol{\beta}\|_\infty$, i.e.,*

$$\|F'_{\boldsymbol{\omega}}(\boldsymbol{\beta}) - F'_{\boldsymbol{\omega}}(\boldsymbol{\beta}')\|_\Phi \leq \kappa\gamma^T \|\boldsymbol{\beta} - \boldsymbol{\beta}'\|_\Phi,$$

where $\boldsymbol{\beta}, \boldsymbol{\beta}' \in \mathbb{R}^M$. Therefore, there exists a fixed point $\boldsymbol{\beta}^*$ of $F'_{\boldsymbol{\omega}}$.

Proof. The proof follows Theorem 3a of Tsitsiklis and Van Roy (1996). We include the steps here in our notation for completeness:

$$\|F'_{\boldsymbol{\omega}}(\boldsymbol{\beta}) - F'_{\boldsymbol{\omega}}(\boldsymbol{\beta}')\|_\Phi = \|(\Phi^\dagger \circ F_{\boldsymbol{\omega}} \circ \Phi)(\boldsymbol{\beta}) - (\Phi^\dagger \circ F_{\boldsymbol{\omega}} \circ \Phi)(\boldsymbol{\beta}')\|_\Phi$$

$$\begin{aligned}
&= \left\| \Phi(\Phi^\dagger \circ F_\omega \circ \Phi)(\beta) - \Phi(\Phi^\dagger \circ F_\omega \circ \Phi)(\beta') \right\|_\infty \\
&\leq \kappa \left\| F_\omega(\Phi\beta) - F_\omega(\Phi\beta') \right\|_\infty \\
&\leq \kappa\gamma^T \left\| \Phi\beta - \Phi\beta' \right\|_\infty \\
&= \kappa\gamma^T \left\| \beta - \beta' \right\|_\Phi,
\end{aligned}$$

where first inequality follows by Lemma E.1 and the second inequality follows by the γ^T -contraction property of F_ω . \square

Lemma E.6. *Let ω^* be the solution of the lower level of FSAVI and let β^* be the fixed point of F'_{ω^*} . The approximate value iteration of the upper level of FSAVI, which produces β_k , has a “value iteration” error of:*

$$\left\| \hat{V}(\beta_k) - \hat{V}(\beta^*) \right\|_\infty \leq (\kappa\gamma^T)^k \frac{\kappa^2 - \kappa^2(\kappa\gamma)^{T+1}}{(1 - \kappa\gamma^T)(1 - \kappa\gamma)} r_{\max}.$$

Proof. We have:

$$\begin{aligned}
\left\| \hat{V}(\beta_k) - \hat{V}(\beta^*) \right\|_\infty &= \left\| \Phi F'_{\omega^*} \beta_{k-1} - \Phi F'_{\omega^*} \beta^* \right\|_\infty \\
&= \left\| F'_{\omega^*} \beta_{k-1} - F'_{\omega^*} \beta^* \right\|_\Phi \\
&\leq \kappa\gamma^T \left\| \Phi\beta_{k-1} - \Phi\beta^* \right\|_\infty \\
&\leq \kappa\gamma^T \left\| \hat{V}(\beta_{k-1}) - \hat{V}(\beta^*) \right\|_\infty \\
&\leq (\kappa\gamma^T)^k \left\| \hat{V}(\beta_0) - \hat{V}(\beta^*) \right\|_\infty \\
&\leq (\kappa\gamma^T)^k \frac{\kappa^2 - \kappa^2(\kappa\gamma)^{T+1}}{(1 - \kappa\gamma^T)(1 - \kappa\gamma)} r_{\max}.
\end{aligned}$$

The first inequality is by Lemma E.5 and the last inequality follows from $\beta_0 = 0$ and Lemma E.4. \square

Lemma E.7. *Consider any ω . If β^* is the fixed point of F'_ω , i.e., $\beta^* = F'_\omega \beta^*$, which exists by Lemma E.5, then it holds that*

$$\left\| V_\omega^* - \hat{V}(\beta^*) \right\|_\infty \leq \left(\frac{1 + \kappa}{1 - \kappa\gamma^T} \right) \varepsilon_{\text{up}}$$

where V_{ω}^* is the fixed point of F_{ω} .

Proof. Let $\varepsilon' = \varepsilon_{\text{up}} + \delta$ for some $\delta > 0$. Choose $\bar{\beta} \in \mathbb{R}^M$ such that $\|V_{\omega}^* - \hat{V}(\bar{\beta})\|_{\infty} < \varepsilon'$. Then,

$$\begin{aligned} \|\hat{V}(\bar{\beta}) - \Phi F'_{\omega}(\bar{\beta})\|_{\infty} &= \|\Phi \bar{\beta} - \Phi \Phi^{\dagger} F_{\omega} \hat{V}(\bar{\beta})\|_{\infty} \\ &= \|\Phi \Phi^{\dagger} \Phi \bar{\beta} - \Phi \Phi^{\dagger} F_{\omega} \hat{V}(\bar{\beta})\|_{\infty} \\ &< \kappa \|\Phi \bar{\beta} - F_{\omega} \hat{V}(\bar{\beta})\|_{\infty} \end{aligned} \tag{44}$$

$$\begin{aligned} &= \kappa \|\hat{V}(\bar{\beta}) - F_{\omega} \hat{V}(\bar{\beta})\|_{\infty} \\ &\leq \kappa \left(\|\hat{V}(\bar{\beta}) - V_{\omega}^*\|_{\infty} + \|V_{\omega}^* - F_{\omega} \hat{V}(\bar{\beta})\|_{\infty} \right) \\ &< \kappa \left(\varepsilon' + \|F_{\omega} V_{\omega}^* - F_{\omega} \hat{V}(\bar{\beta})\|_{\infty} \right) \\ &< \kappa (\varepsilon' + \gamma^T \varepsilon') = \kappa (1 + \gamma^T) \varepsilon', \end{aligned} \tag{45}$$

where (44) is by Lemma E.1 and (45) is by the γ^T -contraction property of F_{ω} . Now, we let $\varepsilon'' = \kappa(1 + \gamma^T) \varepsilon'$ and see that

$$\begin{aligned} \|\hat{V}(\bar{\beta}) - \hat{V}(\beta^*)\|_{\infty} &\leq \|\hat{V}(\bar{\beta}) - \Phi F'_{\omega}(\bar{\beta})\|_{\infty} + \|\Phi F'_{\omega}(\bar{\beta}) - \hat{V}(\beta^*)\|_{\infty} \\ &< \varepsilon'' + \|\Phi \Phi^{\dagger} F_{\omega} \hat{V}(\bar{\beta}) - \Phi \Phi^{\dagger} F_{\omega} \hat{V}(\beta^*)\|_{\infty} \\ &< \varepsilon'' + \kappa \|F_{\omega} \hat{V}(\bar{\beta}) - F_{\omega} \hat{V}(\beta^*)\|_{\infty} \\ &\leq \varepsilon'' + \kappa \gamma^T \|\hat{V}(\bar{\beta}) - \hat{V}(\beta^*)\|_{\infty}. \end{aligned}$$

It thus follows that

$$\|\hat{V}(\bar{\beta}) - \hat{V}(\beta^*)\|_{\infty} \leq \frac{\kappa + \kappa \gamma^T}{1 - \kappa \gamma^T} \varepsilon'.$$

Putting the pieces together, we have

$$\begin{aligned} \|V_{\omega}^* - \hat{V}(\beta^*)\|_{\infty} &\leq \|V_{\omega}^* - \hat{V}(\bar{\beta})\|_{\infty} + \|\hat{V}(\bar{\beta}) - \hat{V}(\beta^*)\|_{\infty} \\ &\leq \varepsilon' + \frac{\kappa + \kappa \gamma^T}{1 - \kappa \gamma^T} \varepsilon' \\ &\leq \frac{1 + \kappa}{1 - \kappa \gamma^T} \varepsilon'. \end{aligned}$$

Since δ can be arbitrarily small, the proof is complete. \square

E.2 Proof of Theorem 8.1

We apply Lemma 5.1 with $\pi = \hat{\pi}_{\omega^*}$, $J_1 = \hat{J}_1(\omega^*)$, and $V = \hat{V}(\beta_k)$. First, to compute the reward error $\epsilon_r(\pi^*, \hat{J}_1(\omega_1^*))$, we have

$$\begin{aligned} \epsilon_r(\pi^*, \hat{J}_1(\omega_1^*)) &= \max_{s,a} |\mathbb{E}[R(s, a, \pi^*)] - \mathbb{E}[\tilde{R}(s, a, \hat{J}_1(\omega_1^*))]| \\ &\leq \epsilon_r(\gamma, \alpha, d_{\mathcal{Y}}, \mathbf{L}, T) + \max_{s,a} |\mathbb{E}[\tilde{R}(s, a, J_1^*)] - \mathbb{E}[\tilde{R}(s, a, \hat{J}_1(\omega_1^*))]| \\ &\leq \epsilon_r(\gamma, \alpha, d_{\mathcal{Y}}, \mathbf{L}, T) + \gamma \|J_1^* - \hat{J}_1(\omega_1^*)\|_{\infty} \\ &\leq \epsilon_r(\gamma, \alpha, d_{\mathcal{Y}}, \mathbf{L}, T) + \left(\gamma + (\gamma + 1) \sum_{i=1}^{T-1} (\gamma')^i \right) \epsilon_{\text{low}}, \end{aligned}$$

where the last inequality follows from Lemma E.3. The other term to analyze is $\|V_{\omega^*}^* - \hat{V}(\beta_k)\|_{\infty}$, where we remind the reader of our usage of the shorthand notation $V_{\omega^*}^* = V^*(\hat{J}_1(\omega^*), \hat{\pi}_{\omega^*})$:

$$\begin{aligned} \|V_{\omega^*}^* - \hat{V}(\beta^*)\|_{\infty} &\leq \|V_{\omega^*}^* - \hat{V}(\beta^*)\|_{\infty} + \|\hat{V}(\beta^*) - \hat{V}(\beta_k)\|_{\infty} \\ &\leq \left(\frac{1 + \kappa}{1 - \kappa\gamma^T} \right) \epsilon_{\text{up}} + (\kappa\gamma^T)^k \left(\frac{\kappa^2 - \kappa^2(\kappa\gamma)^{T+1}}{(1 - \kappa\gamma^T)(1 - \kappa\gamma)} \right) r_{\text{max}}, \end{aligned}$$

which follows by Lemmas E.4 and E.6. This completes the proof.

F Bounds on L_U in Terms of L_r and L_f

We start with an assumption that, if true, leads to a simple bound on the Lipschitz constant L_U . The main result is in Proposition F.1.

Assumption 5. *Suppose that $\gamma L_f < 1$, where the constant L_f , as defined in (3), is the sensitivity of the transition function to small changes in (s, a) .*

Lemma F.1. *Consider an $(\alpha, d_{\mathcal{Y}})$ -fast-slow MDP $\langle \mathcal{S}, \mathcal{A}, \mathcal{W}, f, r, \gamma \rangle$ and let $U : \mathcal{S} \rightarrow \mathbb{R}$ be a value function such that there exists $L_U > 0$ where for any states s and \tilde{s} ,*

$$|U(s) - U(\tilde{s})| \leq L_U \|s - \tilde{s}\|_2. \quad (46)$$

Define the state-action value function $Q(s, a) = r(s, a) + \gamma \mathbb{E}[U(f(s, a, w))]$. Then, for any state-

action pairs (s, a) and (\tilde{s}, \tilde{a}) , the state-action value function Q satisfies

$$|Q(s, a) - Q(\tilde{s}, \tilde{a})| \leq (L_r + \gamma L_U L_f) (\|s - \tilde{s}\|_2 + \|a - \tilde{a}\|_2).$$

Proof. For any state-action pairs $(s, a), (\tilde{s}, \tilde{a}) \in \mathcal{S} \times \mathcal{A}$, we have

$$\begin{aligned} |Q(s, a) - Q(\tilde{s}, \tilde{a})| &\leq |r(s, a) - r(\tilde{s}, \tilde{a})| + \gamma |\mathbb{E}[U(f(s, a, w)) - U(f(\tilde{s}, \tilde{a}, w))]| \\ &\leq L_r (\|s - \tilde{s}\|_2 + \|a - \tilde{a}\|_2) + \gamma L_U \max_w \|f(s, a, w) - f(\tilde{s}, \tilde{a}, w)\|_2 \end{aligned} \quad (47)$$

$$\leq L_r (\|s - \tilde{s}\|_2 + \|a - \tilde{a}\|_2) + \gamma L_U L_f (\|s - \tilde{s}\|_2 + \|a - \tilde{a}\|_2) \quad (48)$$

$$\leq (L_r + \gamma L_U L_f) (\|s - \tilde{s}\|_2 + \|a - \tilde{a}\|_2),$$

where (47) follows by (46) and (48) follows by the definition of L_f in (3). \square

Lemma F.2. Consider an (α, d_Y) -fast-slow MDP $\langle \mathcal{S}, \mathcal{A}, \mathcal{W}, f, r, \gamma \rangle$. Let $Q : \mathcal{S} \times \mathcal{A} \rightarrow \mathbb{R}$ be a state-action value function and assume there exists $L_Q > 0$ where for any states (s, a) and (\tilde{s}, \tilde{a}) ,

$$|Q(s, a) - Q(\tilde{s}, \tilde{a})| \leq L_Q (\|s - \tilde{s}\|_2 + \|a - \tilde{a}\|_2). \quad (49)$$

Define $U(s) = \max_a Q(s, a)$. Then, for any states s and \tilde{s} , the value function U satisfies

$$|U(s) - U(\tilde{s})| \leq L_Q \|s - \tilde{s}\|_2.$$

Proof. Note that:

$$\begin{aligned} |U(s) - U(\tilde{s})| &= \left| \max_a Q(s, a) - \max_{\tilde{a}} Q(\tilde{s}, \tilde{a}) \right| \\ &\leq \max_a |Q(s, a) - Q(\tilde{s}, a)| \\ &\leq L_Q \|s - \tilde{s}\|_2, \end{aligned}$$

where the last inequality is by (49). \square

Lemma F.3. Consider an (α, d_Y) -fast-slow MDP $\langle \mathcal{S}, \mathcal{A}, \mathcal{W}, f, r, \gamma \rangle$. Starting with $U_0 = 0$, recur-

sively define Q_{k+1} and U_{k+1} as follows:

$$Q_{k+1}(s, a) = r(s, a) + \gamma \mathbb{E}[U_k(f(s, a, w))] \quad \text{and} \quad U_{k+1}(s) = \max_a Q_{k+1}(s, a).$$

Then U_k is Lipschitz continuous and its Lipschitz constant L_{U_k} satisfies

$$L_{U_k} = L_r + \gamma L_f L_{U_{k-1}}. \tag{50}$$

Proof. The proof is by induction. For $k = 1$, note that $Q_1(s, a) = r(s, a)$ and therefore has Lipschitz constant L_r by (2). By Lemma F.2, it follows that U_1 also has Lipschitz constant L_r . Since $L_{U_0} = 0$, we see that $L_{U_1} = L_r$ satisfies (50). Now, assume that L_{U_k} satisfies (50) for $k \geq 1$. Then, by Lemma F.1, Q_{k+1} is $(L_r + \gamma L_f L_{U_k})$ -Lipschitz continuous and by Lemma F.2, U_{k+1} is $(L_r + \gamma L_f L_{U_k})$ -Lipschitz continuous. \square

Proposition F.1. Consider an (α, d_Y) -fast-slow MDP $\langle \mathcal{S}, \mathcal{A}, \mathcal{W}, f, r, \gamma \rangle$ and suppose Assumption 5 holds. Then, the optimal value U^* , as defined in (5), satisfies:

$$|U^*(s) - U^*(\tilde{s})| \leq \frac{L_r}{1 - \gamma L_f} \|s - \tilde{s}\|_2$$

for any states $s, \tilde{s} \in \mathcal{S}$.

Proof. According to Proposition 7.3.1 of Bertsekas (2012), the value U_k in Lemma F.3 converges to the optimal value U^* (value iteration). The recursion (50) can be written as:

$$L_{U_k} = L_r + \gamma L_f L_r + \cdots + (\gamma L_f)^{k-1} L_r = \sum_{i=0}^{k-1} (\gamma L_f)^i L_r,$$

a convergent sequence since Assumption 5 is satisfied. Letting $k \rightarrow \infty$, we see that U^* has Lipschitz constant

$$\lim_{k \rightarrow \infty} L_{U_k} = \sum_{i=0}^{\infty} (\gamma L_f)^i L_r = \frac{L_r}{1 - \gamma L_f},$$

completing the proof. \square